J. Med. Chem. **2007,** *50,* 6519–6534

Nonsteroidal Glucocorticoid Agonists: Tetrahydronaphthalenes with Alternative Steroidal A-Ring Mimetics Possessing Dissociated (Transrepression/Transactivation) Efficacy Selectivity

Keith Biggadike, Mohamed Boudjelal, Margaret Clackers, Diane M. Coe, Derek A. Demaine, George W. Hardy, Davina Humphreys, Graham G. A. Inglis, Michael J. Johnston, Haydn T. Jones, David House, Richard Loiseau, Deborah Needham, Philip A. Skone, Iain Uings, Gemma Veitch, Gordon G. Weingarten, Iain M. McLay, and Simon J. F. Macdonald*

ri CEDD, GlaxoSmithKline Medicines Research Centre, Gunnels Wood Road, Stevenage SG1 2NY, U.K.

Received June 29, 2007

The synthesis and biological activity of tetrahydronaphthalene derivatives coupled to various heterocycles are described. These compounds are potent glucocorticoid receptor agonists with efficacy selectivity in an NFκB glucocorticoid receptor (GR) agonist assay (representing transrepression effects) over an MMTV GR agonist assay (representing transactivation effects). Quinolones, indoles, and C- and N-linked quinolines are some of the heterocycles that provide efficacy selectivity. For example, the isoquinoline **49D1E2** has NFκB agonism with pIC_{50} of 8.66 (89%) and reduced efficacy in MMTV agonism (6%), and the quinoline **55D1E1** has NFκB agonism with pIC_{50} of 9.30 (101%) and reduced efficacy in MMTV agonism with pEC_{50} of 8.02 (47%). A description of how a compound from each class is modeled in the active site of the receptor is given.

Introduction

Glucocorticoid agonists have been used for many years as anti-inflammatory agents for treating a whole spectrum of conditions including asthma and rheumatoid arthritis.[1] Fluticasone propionate **1** (Figure 1) is commonly used as a safe and effective inhaled treatment for asthma. In contrast, dexamethasone **2** and prednisolone **3** are commonly prescribed oral treatments for rheumatoid arthritis. Mifepristone **4** (RU486) is a standard glucocorticoid antagonist. About 10 million prescriptions are written each year for oral glucocorticoid agonists in the U.S. alone, and it is estimated that well over 50% of patients with rheumatoid arthritis are treated more or less continuously with glucocorticoid agonists.[2] Overall, the market size for all uses of glucocorticoids is estimated as \$10 billion per year.[3] However, prolonged use of orally administered glucocorticoid agonists in the treatment of chronic conditions is blighted by serious and unpleasant side effects including, among many others, glucose intolerance, muscle wasting, skin thinning, and osteoporosis.[3]

As a consequence of these side effects, there has recently been considerable interest in a hypothesis of selective glucocorticoid agonism where the beneficial anti-inflammatory effects are postulated to be derived from transrepression (TR) pathways and may be separated from the side effects derived from transactivation (TA) pathways.[4] Compounds which display selectivity for transrepression over transactivation are often referred to as dissociated agonists. Lucid descriptions of the molecular basis for these pathways have been described in detail elsewhere.[2–4] Recent publications have described nonsteroidal structures that are both dissociated glucocorticoid receptor (GR[a]) agonists that feature TR/TA selectivity[5–9] and GR antagonists.[10,11]

At GSK, we are interested in GR agonists as anti-inflammatory agents and have recently described nonsteroidal GR modulators designed by using an agreement docking method.[12–14]

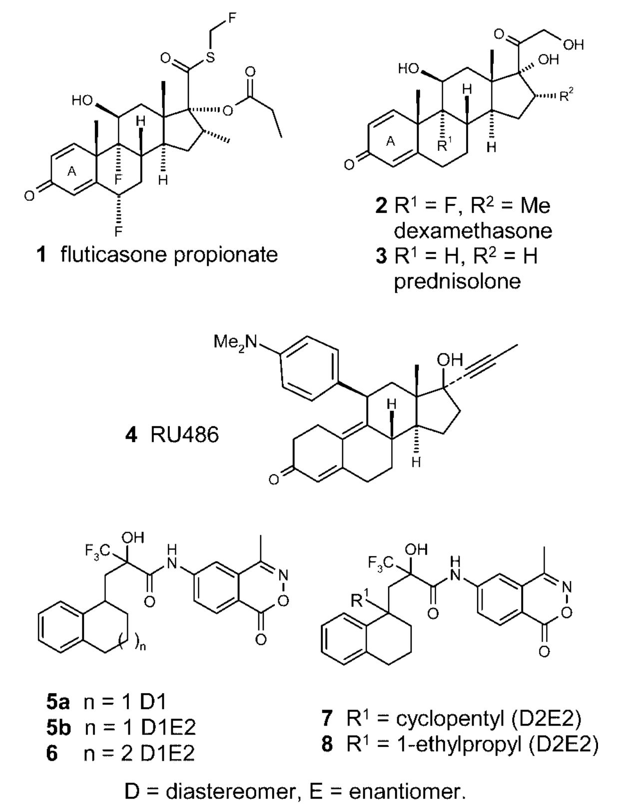

Figure 1. Steroidal (**1–4**) and nonsteroidal glucorticoid agonists (**5–8**).

These modulators, exemplified by **5a**, **5b**, and **6**, are potent binders to GR with the IC_{50} value of **6** in the NFkB assay being submicromolar. We were subsequently able to convert these analogues into potent full agonists of GR possessing indications of dissociation (that is, selectivity for transrepression over transactivation) through the discovery of an "agonist trigger".[14] In **7** and **8**, the agonist trigger is the cyclopentyl and 1-ethylpropyl R^1 group. Compounds such as **7** and **8** are GR agonists

* To whom correspondence should be addressed. Fax: 44 1438-768-302. E-mail: simon.jf.macdonald@gsk.com.

[a] Abbreviations: GR, glucocorticoid receptor; NFκB, nuclear factor κB; MMTV, mouse mammary tumor virus; SAR, structure–activity relationship.

10.1021/jm070778w CCC: \$37.00
Published on Web 11/27/2007

Scheme 1[a]

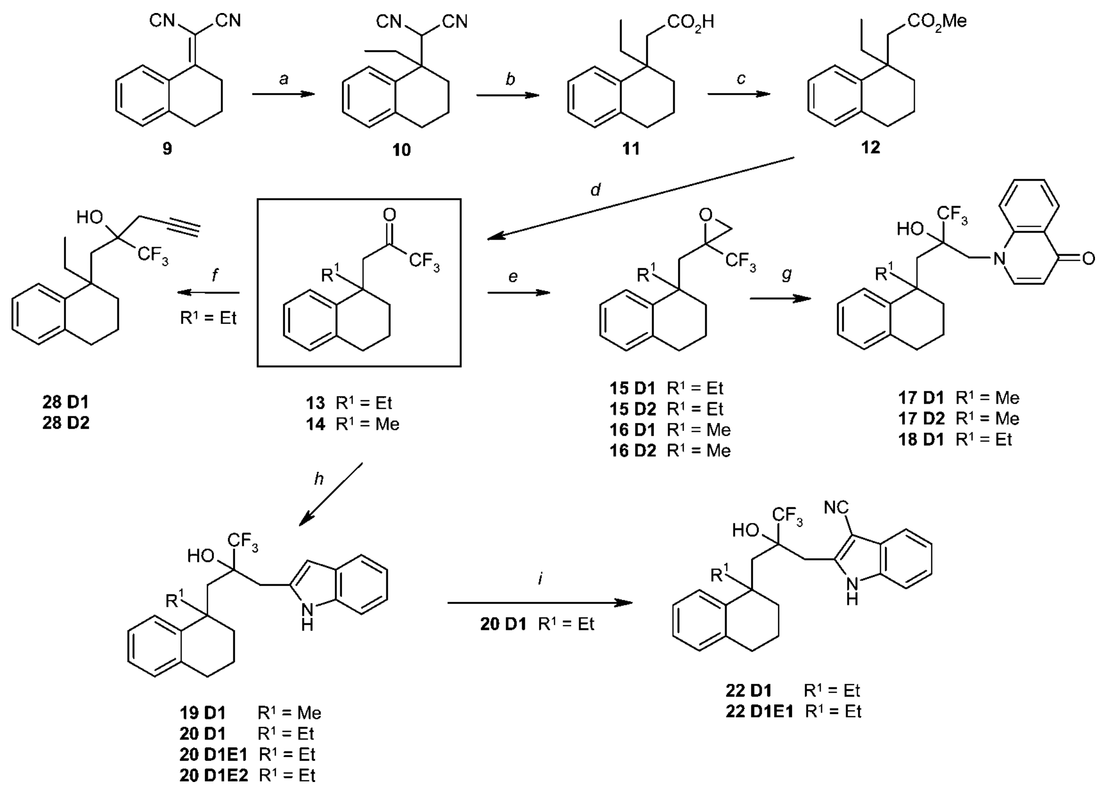

[a] Reagents and conditions: (a) EtMgBr, CuI, THF, reflux; (b) KOH, ethylene glycol, reflux; (c) MeI, K_2CO_3, Me_2CO, reflux; (d) $KN(SiMe_3)_2$, CHF_3, DMF, −10°C; (e) NaH, $Me_3SO^+I^-$, DMSO, THF, room temp; (f) $BrCH_2CCSiMe_3$, Rieke zinc, $HgCl_2$, THF and then TBAF, THF, room temp; (g) 4-hydroxyquinoline, KO*t*Bu, DMF, room temp; (h) 2-methylindole, *n*BuLi, KO*t*Bu, THF, −70°C; (i) $ClSO_2NCO$, DMF, MeCN, 5°C.

with potency similar to that of dexamethasone with activity in a mouse delayed hypersensitivity model after topical treatment.[14]

All the tetrahydronaphthalene compounds described so far feature the 5-aminobenzoxazinone moiety which, from modeling studies, acts as the steroidal A-ring mimetic.[12,14] While many of these compounds are both potent and TR/TA efficacy selective, the presence and reactivity of the benzoxazinone moiety severely limit the chemistry that can be performed elsewhere in the molecule. Further, in vitro studies with rat and human liver microsomes indicate that this group is readily metabolized and, thus for use as an oral therapy, requires replacing. We were also interested in exploring the structure–activity relationships (SAR) of benzoxazinone replacements with readouts of transrepression and transactivation.

We describe in this paper analogues featuring replacements of the benzoxazinone that both maintain GR agonist potency and show outstanding efficacy selectivity in transrepression and transactivation assays. We again demonstrate that in this tetrahydronaphthalene series, the R^1 group (as described above for **7** and **8**) is a key substituent[14] that acts as an "agonist trigger", but the nature of the most preferred R^1 group varies depending on the nature of the benzoxazinone replacement. From modeling studies, we also show how representative examples of different benzoxazinone replacements might bind in the active site of GR.

Chemistry

To simplify comparison of the various isomeric analogues of compounds containing two chiral centers, in the absence of being able to assign the absolute stereochemistry, each parent compound has a unique number followed by a consistent arbitrary isomeric assignment. Thus, **45D1** refers to compound **45**, racemic diastereomer 1; **45D1E1** refers to compound **45**, diastereomer 1, enantiomer 1; **45D1E2** refers to compound **45**, diastereomer 1, enantiomer 2; and so forth. In some cases the racemic mixtures of diastereomers were not separated, and here, these are referred to as **46D1+D2**. Where diastereomers were prepared in the same reaction, the first eluting diastereomer on LC/MS is defined as diastereomer 1 and the second eluting isomer as diastereomer 2. Within a series, comparison of diagnostic ^1H NMR peaks for diastereomer 1 analogues suggests that the relative stereochemistry remains constant and similarly for diastereomer 2. Enantiomers are named on the basis of the order of elution from the analytical chiral HPLC column; thus, enantiomer 1 is the first eluting isomer and enantiomer 2, is the second eluting isomer. No conclusions are drawn in relating the absolute stereochemistry of enantiomers of analogues even when closely related and purified using the same chiral HPLC column.

The key intermediates for preparing the targets for testing were variously R^1 substituted tetrahydronaphthalene trifluoromethyl ketones (**13**, **14**, **39**), trifluoromethyl epoxides (**15**, **16**), and trifluoromethylhydroxy aldehydes (**47**, **53**). The R^1 = Et trifluoromethylketone **13** was prepared from the dinitrile **9** in a four-step sequence (Scheme 1). Conjugate addition to **9** using ethylmagnesium cuprate was followed by hydrolysis and decarboxylation to afford acid **11**. (Conjugate addition to the analagous malonate failed.) Following esterification, conversion to the trifluoromethylketone **13** was achieved with fluoroform and potassium bis(trimethylsilyl)imide in DMF at −10 °C overnight in 85% yield. Warmer conditions can lead to addition of a further trifluoromethyl group. Other trifluoromethylation conditions either failed or gave much poorer yields. The R^1 = Me analogue **14** may be prepared similarly or using a route similar to that of the R^1 = cyclopentyl analogue **39** (see later). Treatment of the trifluoromethylketones **13** or **14** with sodium

Scheme 2[a]

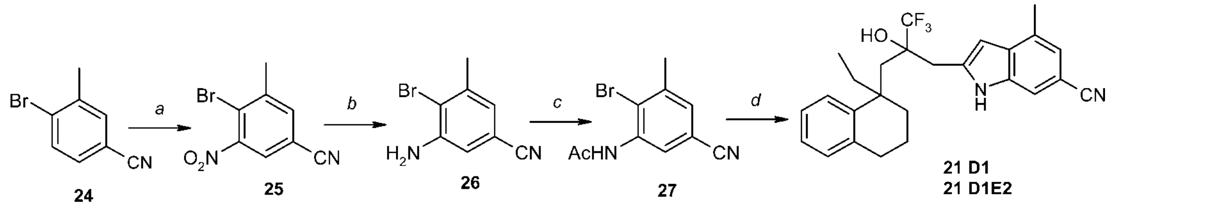

[a] Reagents and conditions: (a) concentrated H_2SO_4, concentrated HNO_3, <15°C; (b) $SnCl_2$, THF, 60–90°C and then Fe, HCl (aq); (c) Ac_2O, 80–100°C; (d) **28D1**, CuI, tetramethylguanidine, dioxane, $(Ph_3P)_2PdCl_2$, 80°C.

Scheme 3[a]

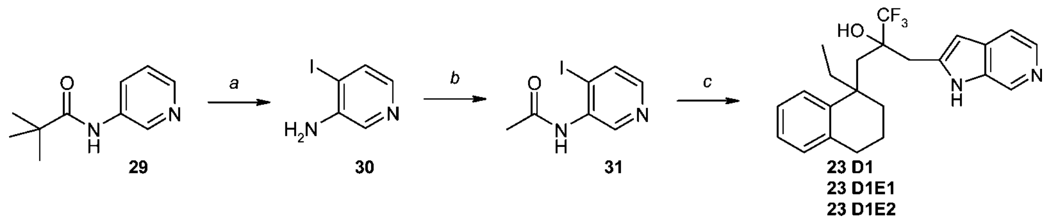

[a] Reagents and conditions: (a) *n*BuLi, TMEDA, THF, −70°C, then I_2, then 24% H_2SO_4, reflux; (b) Ac_2O, pyridine, 60–90°C; (c) **28D1**, CuI, tetramethylguanidine, dioxane, $(Ph_3P)_2PdCl_2$, 80°C.

hydride and trimethylsulfoxonium iodide furnished 2:1 ratios of the epoxide diastereomers **15D1**, **15D2**, **16D1**, and **16D2**, which can be separated by chromatography. Reaction of 4-hydroxyquinoline with potassium *tert*-butoxide and the appropriate epoxide gave the quinolones **17D1**, **17D2**, and **18D1**. Deprotonation of 2-methylindole with a mixture of potassium *tert*-butoxide and *n*-butyllithium followed by treatment with the trifluoromethylketones **13** or **14** gave the indole products **19D1** and **20D1** (and its enantiomers **20D1E1** and **20D1E2**). Cyanation of **20D1** with chlorosulfonyl isocyanate gave the 3-cyanoindole products **22D1** and the enantiomer **22D1E1** in low yield.

The substituted indole **21** (Scheme 2) and azaindole **23** (Scheme 3) were prepared by construction of the heterocycle. Thus, conversion of the trifluoromethylketone **13** into the acetylene derivative **28** was achieved using an alkynyl reagent generated from 3-bromoprop-1-ynyltrimethylsilane, Rieke zinc, and mercuric chloride, followed by desilylation with tetrabutylammonium fluoride. Separation into the corresponding diastereomers (generated in a 2:1 ratio) required exhaustive chromatography. Reaction of **28D1** with either **27** or **31** (prepared using standard protocols; see Schemes 2 and 3) yielded **21D1** (and its enantiomer **21D1E1**) or **23D1** (and its enantiomers **23D1E1** and **23D1E2**), respectively, in low yield.

Preparation of the C-linked quinolines used the trifluoromethylketones **13**, **14**, and **39**. The R^1 = Me ketone **14** and the R^1 = cyclopentyl ketone **39** were similarly prepared with the synthetic sequence for the latter, exemplified in Scheme 4. The sequence starts from the olefin **37**, which was prepared in one pot using 2-iodobenzylzinc bromide, acryloyl chloride, and a cyclopentylzinc bromide as described previously.[14] Palladium mediated intramolecular cyclization of **37** followed by in situ trapping with tributyl(1-(trifluoromethyl)ethenyl)stannane **36** gave the trifluoromethyl olefin **38**, which was converted into the trifluoromethylketone **39** by ozonolysis (33% yield for the two steps).

The trifluoromethylketones **13**, **14**, and **39** were converted into the C-linked quinolines derivatives **33D1** (and its enantiomer **33D1E1**), **35D1**, **40D2**, **41D1**, and **41D2** by treatment with the anion of the 4-methylquinoline or 2-chloro-4-methylquinoline in reasonable yields. Generally one diastereomer is generated in preference to or to the exclusion of the other.

Scheme 4[a]

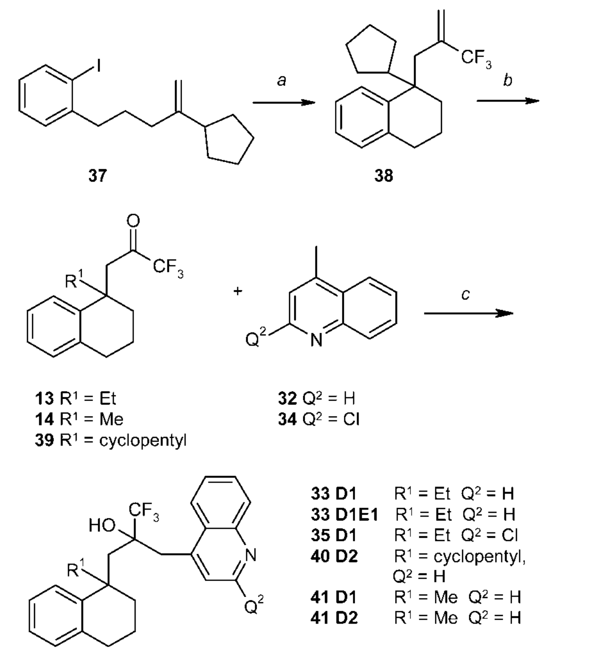

[a] Reagents and condtions: (a) **36**, $Pd(OAc)_2$, CuI, Ph_3P, DMF, 110°C; (b) O_3, MeOH, −70°C to room temp, then Me_2S; (c) **32** or **34**, LDA, THF, then add **13**, **14**, or **39**, −70 to −10 °C.

The N-linked quinolines were prepared by reductive amination of diastereomeric mixtures of the aldehydes **47** and **53** (Scheme 5). The synthetic sequence, exemplified for the R^1 = Me analogues, started from the acyclic olefin **50**.[14] Cyclization to the tetrahydronaphthalene **51** (as described for the transformation above of **37** into **38**) was followed by dihydroxylation with AD-mix α and AD-mix *β* to give **52**. Subsequent oxidation with pyridine/sulfur trioxide complex afforded the aldehydes as a mixture of diastereomers. Two-stage reductive aminations were effected; initially the imines were formed by treatment of the aldehydes with the 5-aminoquinolines or isoquinolines using microwave irradiation at 150 °C. Following workup, reduction of the imines was achieved with sodium triacetoxyborohydride to give separable mixtures of the target compounds **43D2**, **45D1**

Scheme 5[a]

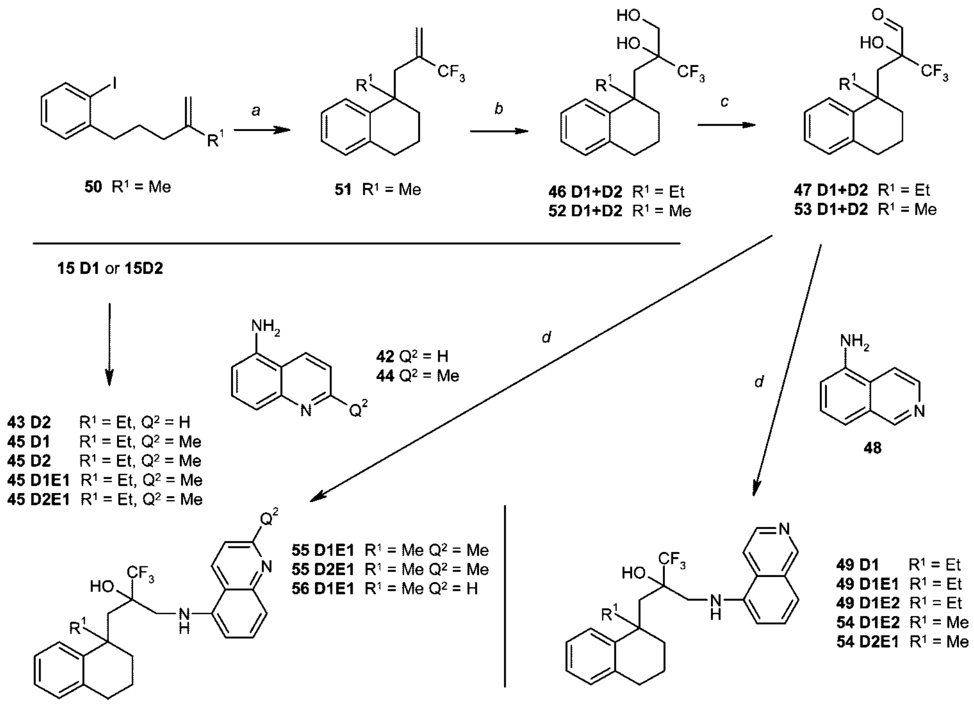

[a] Reagents and conditions: (a) **36**, $Pd(OAc)_2$, CuI, Ph_3P, DMF, 110°C; (b) AD-mix α, AD-mix *β*, ^{t}BuOH, H_2O, 40°C; (c) pyridine–SO_3 complex, Et_3N, CH_2Cl_2, DMSO, 8°C to room temp; (d) **47** or **53** with **42**, **44**, or **48**, AcOH, microwave, 150 °C, then $NaBH(OAc)_3$, AcOH, room temp; (e) **42** or **44**, KO^{t}Bu, DMA, room temp.

(and **45D1E1**), **45D2** (and **45D2E1**), **49D1** (and **49D1E1** and **49D1E2**), **54D1E2**, **54D2E1**, **55D1E1**, **55D2E1**, and **56D1E1**.

Biological Assays

GR Binding Assay. The compounds were tested for their ability to bind to GR using competition experiments with fluorescent-labeled dexamethasone.[12] The tight binding limit of the assay is about $pIC_{50} = 8.5$.

GR NF*κ*B Functional Agonist Assay (Transrepression). A functional GR agonist assay was carried out using human A549 lung epithelial cells engineered to contain a secreted placental alkaline phosphatase gene under the control of the distal region of the NF*κ*B dependent ELAM promoter.[14] This assay allows determination of the ability of compounds to repress transcription (i.e., transpression). Efficacy is expressed as a percentage of the dexamethasone response.

GR MMTV Functional Assay (Transactivation). Human A549 lung epithelial cells were engineered to contain a renilla luciferase gene under the control of the distal region of the LTR from the mouse mammary tumor virus as previously described.[14] While the standards dexamethasone **2** and prednisolone **3** have comparable efficacy in the NF*κ*B transrepression agonist assay and the MMTV transactivation agonist assay, they are more potent in the NF*κ*B assay by about 0.4–0.6 pIC_{50} units. This assay also allows determination of the ability of compounds to activate transcription (i.e., transactivation).

GR MMTV Antagonist Assay. The GR antagonist assay also used human A549 lung epithelial cells stably transfected with the mouse mammary tumor virus (MMTV) luciferase reporter gene. Compounds were tested for their ability to antagonize dexamethasone-induced activation.[14]

Data for target compounds and standards (dexamethasone for agonism and mifepristone (RU486) **4** for antagonism) in these assays are reported.

Results

The aim of our research at GlaxoSmithKline was to identify a new glucocorticoid agonist that can be used as an anti-inflammatory and possesses a reduced side effect profile. Clinical studies will be ultimately required to determine what transrepression efficacy and potency (the NF*κ*B readout) profile is consistent with useful anti-inflammatory activity and what transactivation efficacy and potency (the MMTV agonist and antagonist readout) profile will deliver significant reduction in clinically observed side effects. In the interim, it was therefore of great interest to obtain compounds possessing a variety of profiles in the NF*κ*B and MMTV in vitro assays for further study in phenotypic in vitro assays and in vivo models. Two profiles were of particular interest. The first was an agonist showing efficacy selectivity for transrepression (potent and with high efficacy (>80%) in NF*κ*B) over transactivation pathways (with lower efficacy (<40%) in the MMTV agonist assay and higher efficacy in the MMTV antagonist assay). The second profile was for a potent partial agonist (40–80%) in both NF*κ*B and MMTV agonist assays.

Previously we have described tetrahydronaphthalene–benzoxazine agonists **7** and **8**,[14] which show some efficacy selectivity in the NF*κ*B assay over the MMTV agonist and significant MMTV antagonist activity (Table 1). These compounds were a result of optimization of the tetrahydronaphthalene portion of the molecule where the nature of the R^1 group proved critical to both potency and selectivity. We describe here a series of analogues where the benzoxazine has been replaced with various heterocycles.

From previous studies,[12,14] the benzoxazinone of **7** and **8** acts as a hydrogen bond acceptor similar to the carbonyl of the

Table 1. Biological Data for Quinolones and Indole Analogues

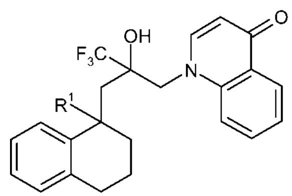

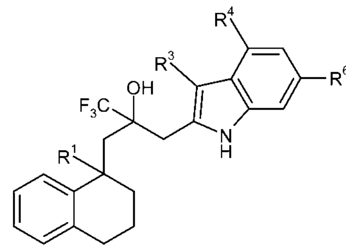

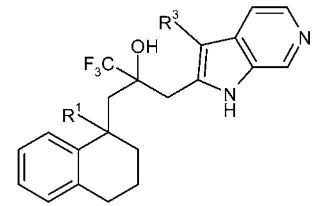

compd[a]	quinolone, indole, or azaindole	stereochem	R^1	R^x	GR binding,[b,c] pIC_{50}	NFκB[b,d] pIC_{50} (% max)	MMTV[b,e] agonism, pEC_{50} (% max)	MMTV[b,f] antagonism, pIC_{50}
Dex **2**					8.10 ± 0.04	8.93 ± 0.07 (110% ± 5)	8.3 ± 0.23 (102% ± 10.8)	<5
Pred **3**					nt[g]	8.07 ± 0.15 (98.4% ± 3.8)	7.50 ± 0.49 (100.3% ± 0.15)	nt[g]
4[h]					8.24 ± 0.09	<6	nt[g]	8.33 ± 0.36 (99.7% ± 0.49)
7					8.09 ± 0.35	8.69 ± 0.45 (92% ± 22)	7.75 ± 0.58 (39% ± 9)	7.27 ± 0.60 (79% ± 22.1)
8					8.28 ± 0.03	8.92 ± 0.25 (105% ± 21)	8.20 ± 0.22 (47% ± 13)	7.18 ± 0.20 (68% ± 18.2)
17D1	quinolone	D1	Me		7.85 ± 0.12	7.31 ± 0.26 (57.8% ± 11.4)	<6 (8.3% ± 2.5)	6.65 ± 0.42 (92.7% ± 4.3)
17D2	quinolone	D2	Me		7.46 ± 0.19	<6 (26.8% ± 6.6%)	<6 (1.9% ± 1.6)	6.15 ± 0.37 (70% ± 1.0)
18D1	quinolone	D1	Et		7.85 ± 0.22	8.09 ± 0.12 (55.1% ± 4.7)	<6 (7.5% ± 1.1)	nt[g]
19D1	indole	D1	Me		7.64 ± 0.23	7.37 ± 0.26 (87.0% ± 8.5)	7.38 ± 0.22 (29.1% ± 5.6)	6.35 ± 0.36 (67.7% ± 6.3)
20D1	indole	D1	Et		7.50 ± 0.25	7.24 ± 0.20 (79.3% ± 12.4)	7.19 ± 0.02 (20.3% ± 3.9)	nt[g]
20D1E1	indole	D1E1	Et		7.85 ± 0.07	7.95 ± 0.05 (84.4% ± 1.2)	7.21 ± 0.03 (17.7% ± 10.1)	6.61 ± 0.31 (77.3% ± 6.3)
20D1E2	indole	D1E2	Et		5.9 ± 0.15	<6 (32.2% ± 4.5)	nt[g]	nt[g]
21D1	indole	D1	Et	4-Me, 6-CN	7.05 ± 0.11	8.14 ± 0.17 (106.8% ± 3.8)	7.23 ± 0.05 (38.4% ± 1.5)	nt[g]
21D1E2	indole	D1E2	Et	4-Me, 6-CN	7.41 ± 0.11	8.42 ± 0.19 (100.3% ± 6.5)	7.29 ± 0.14 (36.4% ± 9.0)	nt[g]
22D1E1	indole	D1E1	Et	3-CN	8.12 ± 0.23	8.18 ± 0.24 (61.1% ± 1.5)	<6 (5.1% ± 1.5)	7.24 ± 0.26 (97.8% ± 3.8)
23D1	azaindole	D1	Et		7.55 ± 0.10	7.7 ± 0.26 (85% ± 4.2)	<6 (9.1% ± 2.6)	nt[g]
23D1E1	azaindole	D1E1	Et		8.05 ± 0.05	8.05 ± 0.24 (82% ± 3.1%)	<6 5.8% ± 5.2)	6.13 ± 0.10 (87.0% ± 3.0)

[a] D = diastereomer, E = enantiomer. The stereochemistry of the diastereomers has been consistently assigned by retention time on LC/MS. Enantiomer assignment is based on the order of elution from analytical chiral HPLC. See text for further details. [b] pIC_{50} values are from duplicate wells with at least $n = 3$ from 11-point dose–response curves with a top concentration of 10 mM. Standard errors are shown. [c] In the GR binding assay, compounds were tested for their ability to bind to GR using competition experiments with fluorescent labeled dexamethasone. [d] The NFκB assay used human A549 lung epithelial cells engineered to contain a secreted placental alkaline phosphatase gene under the control of the distal region of the NFκB dependent ELAM promoter. With a top concentration of 10 mM being tested, pIC_{50} values are not quoted for values less potent than $pIC_{50} = 6$. Maxima are quoted with reference to the maximum for dexamethasone (the standard used). [e] The MMTV transactivation assay human A549 lung epithelial cells were engineered to contain a renialla luciferase gene under the control of the distal region of the LTR from the mouse mammary tumor virus. [f] The GR antagonist assay used human A549 lung epithelial cells stably transfected with the mouse mammary tumor virus (MMTV) luciferase reporter gene. Compounds were tested for their ability to antagonize dexamethasone induced activation. [g] nt = not tested. [h] RU486 (mifepristone) was used as the standard for GR antagonism.

Table 2. Biological Data for C-Linked Quinoline Analogues

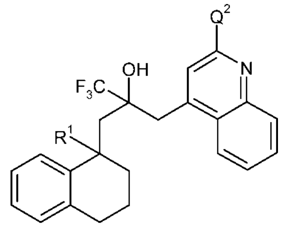

compd[a]	stereochem	R^1	Q^2	GR binding,[b,c] pIC_{50}	NFκB[b,d] pIC_{50} (% max)	MMTV[b,e] agonism, pEC_{50} (% max)	MMTV[b,f] antagonism, pIC_{50}
Dex **2**				8.10 ± 0.04	8.93 ± 0.07 (110% ± 5)	8.3 ± 0.23 (102% ± 10.8)	<5
Pred **3**				nt[g]	8.07 ± 0.15 (98.4% ± 3.8)	7.50 ± 0.49 (100.3% ± 0.15)	nt[g]
4[h]				8.24 ± 0.09	<6	nt[g]	8.33 ± 0.36 (99.7% ± 0.49)
33D1	D1	Et	H	7.82 ± 0.35	8.31 ± 0.14 (84.4% ± 6.3)	7.42 ± 0.11 (12.2% ± 1.1)	5.30 ± 0.15 (63.5% ± 0.55)
33D1E1	D1E1	Et	H	8.0 ± 0.20	8.8 ± 0.10 (83.1% ± 2.5)	<6 (21.5% ± 3.9)	nt[g]
33D2	D2	Et	H	7.48 ± 0.55	6.56 ± 0.21 (72.6 ± 10.7%)	<5 (7.8% ± 4.5)	nt[g]
35D1	D1	Et	Cl	7.55 ± 0.21	7.52 ± 0.19 (67.4 ± 15.4%)	7.29 ± 0.05 (22.5% ± 0.77)	nt[g]
40D2	D2	cyclopentyl	H	6.83 ± 0.39	6.13 ± 0.70 (56.26% ± 5.0)	<5 (1.45% ± 1.8)	nt[g]
41D1	D1	Me	H	7.82 ± 0.29	8.15 ± 0.04 (74.75% ± 2.2)	7.89 ± 0.37 (20.75% ± 1.6)	nt[g]
41D2	D2	Me	H	7.62 ± 0.51	<5 (38.9% ± 6.2)	<5 (6.5% ± 0.56)	nt[g]

[a] D = diastereomer, E = enantiomer. The stereochemistry of the diastereomers has been consistently assigned by retention time on LC/MS. Enantiomer assignment is based on the order of elution from analytical chiral HPLC. See text for further details. [b] pIC_{50} values are from duplicate wells with at least n = 3 from 11-point dose–response curves with a top concentration of 10 mM. Standard errors are shown. [c] In the GR binding assay, compounds were tested for their ability to bind to GR using competition experiments with fluorescent labeled dexamethasone. [d] The NFκB assay used human A549 lung epithelial cells engineered to contain a secreted placental alkaline phosphatase gene under the control of the distal region of the NFκB dependent ELAM promoter. With a top concentration of 10 mM being tested, pIC_{50} values are not quoted for values less potent than pIC_{50} = 6. Maxima are quoted with reference to the maximum for dexamethasone (the standard used). [e] The MMTV transactivation assay human A549 lung epithelial cells were engineered to contain a renialla luciferase gene under the control of the distal region of the LTR from the mouse mammary tumor virus. [f] The GR antagonist assay used human A549 lung epithelial cells stably transfected with the mouse mammary tumor virus (MMTV) luciferase reporter gene. Compounds were tested for their ability to antagonize dexamethasone induced activation. [g] nt = not tested. [h] RU486 (mifepristone) was used as the standard for GR antagonism.

steroidal A-ring (see ring A in **1–3**). Examination of the literature (including the patent literature)[6,8] suggests a plethora of alternative A-ring mimetics. Which of these might offer selectivity for transrepression over transactivation? Unfortunately, in the patent literature there is rarely clear and comprehensive biological data describing the full profile of these alternative A-ring mimetics, and it was therefore of great interest to explore some of these in the tetrahydronaphthalene series. We describe here the incorporation of some of these putative A-ring mimetics, namely, quinolones, indoles, azaindoles, C-linked quinolines, and N-linked quinolines and isoquinolines, into the tetrahydronaphthalene series.

Three quinolones were prepared as potential replacements for the benzoxazinone: **17D1**, **17D2**, and **18D1**. All are good GR binders, but **17D1** (R^1 = Me) is a dissociated agonist (a partial agonist in the NFκB assay and a full antagonist in the MMTV antagonist assay). In contrast, its diastereomer **17D2** shows only antagonist activity. The R^1 ethyl analogue **18D1** shows a similar profile to **17D1** being a partial agonist but with an increased potency of pIC_{50} = 8.09 (55%) in the NFκB assay, which is similar to prednisolone **3** (a full agonist). As will be seen, different racemic diastereomers can display quite different profiles: agonism and antagonism (for example, **17D1** and **17D2** above). However, for an individual diastereomer one enantiomer is generally substantially more active than the other enantiomer (for example, **20D1E1** and **20D1E2**). Thus, it is unlikely (in these series at least) that where the enantiomers have not been separated, they would display significantly profiles different from those observed for the racemic diastereomer.

In contrast to the quinolones, the unsubstituted indole replacements[8] **19D1** and **20D1E1** for the benzoxazinone do not feature an H-bond acceptor (Table 1) (see later). In this series both the R^1 = Me and Et analogues **19D1** and **20D1E1** have similar binding and NFκB agonist activity and display ~55–65% efficacy selectivity over MMTV agonist activity. The indole analogue where R^1 = cyclopentyl, one of the most potent R^1 substituent in the benzoxazinone series, is completely inactive (data not shown). For all the indoles prepared, D1 is more potent than D2 (data not shown) and the active enantiomer of the active diastereomer is much more potent than the other enantiomer (compare **20D1E1** GR binding pIC_{50} = 7.85 with **20D1E2** GR binding pIC_{50} = 5.9). Substitution on the indole ring has an effect on efficacy. Thus, the R^1 = Et 4-methyl-6-cyanoindole analogue[8] **21D1E2** is a slightly fuller and more potent NFκB agonist with ~65% efficacy selectivity over MMTV agonism when compared with the unsubstituted analogue **20D1E1**. In contrast, the 3-cyanoindole analogue[8] **22D1E1** is a much more partial NFκB agonist of pIC_{50} = 8.2 (61%) with ~55% efficacy selectivity over MMTV agonism and a particularly potent MMTV antagonist of pIC_{50} = 7.2 (98%). The azaindole[8] **23D1E1** has a similar level of NFκB potency of pIC_{50} = 8.0 (82%) but has the best efficacy selectivity over MMTV agonism (~75%) in this series. While the nitrile substituted analogues and azaindole feature hydrogen bond acceptor groups, these features appear to have little effect on either the GR binding or NFκB potency (see later for a discussion on how these compounds might bind in the glucocorticoid receptor).

A series of C-linked quinolines were prepared (Table 2). In this series the N of the quinoline is an obvious H-bond acceptor. A variety of R^1 triggers were made, and as for the unsubstituted indoles, the R^1 = Et **33D1** has similar activity to the R^1 = Me **41D1** being potent agonists (NFκB pIC_{50} = 8.1–8.3) with the cyclopentyl analogue **40D2** being much less active (albeit this is likely to be the less active diastereomer, it was not possible to prepare the other diastereomer **40D1** using the described route). The R^1 = H analogue, while binding, has no agonist activity at all (data not shown). As has been described elsewhere[14] and as observed in other series described herein, the presence of the appropriate "agonist trigger" is critical to observing agonism. The molecular interactions between the ligand and the receptor that lead to this sensitivity are not clear from our modeling studies.

Diastereomer 1 analogues are much more superior NFκB agonists compared to the diastereomer 2 analogues (compare **33D1** with **33D2** or **41D1** with **41D2**). 2-Chloro substitution on the quinoline **35D1** lowers the NFκB agonist activity about 5-fold and is a partial agonist ($pIC_{50} = 7.5$ (67%)). (A difference in 0.7 pIC_{50} units equates to a 5-fold difference in nonlogarithmic units.) The best compound in the series is **33D1E1** with NFκB agonist potency approaching dexamethasone-like levels with $pIC_{50} = 8.8$ (83%) and ~70% efficacy selectivity over MMTV agonism.

A series of N-linked quinolines and isoquinolines were also prepared (Table 3). These compounds are slightly longer than the C-linked quinoline series and are linked to the rest of the molecule at C5 of the heterocycle (compared to C4 of the C-linked heterocycles). All of the analogues have good GR binding activity, and diastereomer 1 compounds are more potent NFκB agonists than diastereomer 2 compounds (compare **45D1** with **45D2**, **54D1E2** with **54D2E1**, or **55D1E1** with **55D2E1**). A range of substituents were incorporated at the R^1 position of the tetrahydronaphthalene. The R^1 = Me analogue is slightly more NFκB potent than the Et analogue (compare **45D1E1** with **55D1E1** or **49D1E2** with **54D1E2**) and is much more superior to the R^1 = cyclopentyl analogues, which are typically 10- to 100-fold less active (data not shown). The R^1 = H analogues, while binding, are inactive against NFκB (data not shown). (The same comments made for the R^1 = H C-linked quinolines above also apply here.) Methyl substitution at the 2 position of the quinoline has a major effect in that it significantly increases the NFκB potency and efficacy and decreases the efficacy selectivity over MMTV agonism. Thus, where R^1 = Et, the methyl analogue **45D1** is a full agonist with NFκB $pIC_{50} = 8.6$ (91%) and MMTV agonism $pIC_{50} = 7.9$ (73%) compared with the des-methyl parent compound **43D1**, which is a partial agonist with NFκB $pIC_{50} = 7.9$ (65%) and MMTV agonism $pIC_{50} < 6$ (5%). Similarly, where R^1 = Me, the methyl analogue **55D1E1** is a full agonist with NFκB $pIC_{50} = 9.3$ (101%) and MMTV $pIC_{50} = 8.0$ (48%) compared with the des-methyl parent compound **56D1E1**, which is a partial agonist with NFκB $pIC_{50} = 8.5$ (69%) and MMTV $pIC_{50} = 7.9$ (20%). Substitution at the 2 position of the quinoline with groups larger than a methyl group leads to decreased activity (data not shown). The isoquinoline analogue **54D1E2** (R^1 = Me) is similarly potent in NFκB agonism and efficacy compared to the 2-methylquinoline **55D1E1**. Both the isoquinoline analogues **49D1E2** (R^1 = Et) and **54D1E2** (R^1 = Me) display good to excellent efficacy selectivity for NFκB agonism over MMTV agonism with selectivity differences of 83% and 51%, respectively. The analogues showing the best combination of NFκB potency and efficacy selectivity are the isoquinoline **49D1E2** having NFκB $pIC_{50} = 8.66$ (89%) and MMTV agonism $pIC_{50} < 6$ (6%) and the quinoline **55D1E1** having NFκB $pIC_{50} = 9.30$ (101%), MMTV agonism $pIC_{50} = 8.02$ (47%), and MMTV antagonism $pIC_{50} = 7.11$ (37%).

Discussion

Previously, we had observed that the NFκB potency and efficacy selectivity over MMTV agonism could be obtained by variation of the R^1 group in structures such as **7** and **8**.[14] The modeling of these compounds into the active site of GR has also been described.[14] It is striking that the region of the active site where structural variations in **7** and **8** cause efficacy selectivity is the same region[15] where efficacy selectivity has also been observed for a series of betamethasone 17α-carbamates.[16] This paper describes a new area, namely, the area that binds the heterocycle (which acts as an A-ring mimetic of the steroid), which can also cause efficacy selectivity for NFκB agonism over MMTV agonism.

Previous studies[14] have indicated that the benzoxazinone moiety is a "steroidal A-ring mimetic". To better understand the interactions of the benzoxazinone and several of the described heterocyclic replacements with the protein in this region, some simple mutation studies were performed. The two H-bonding residues Gln570 and Arg611 were mutated singly to Ala, and functional dependence was investigated at a single high concentration of 1 μM (Table 4). These studies will be reported in detail elsewhere. However, it is important to note that these residues were not found to be essential for functional activity; i.e., the mutations do not disrupt the architecture of the protein. For example, the potent steroid fluticasone propionate (typically 2 orders of magnitude more potent than dexamethasone) was able to retain function with either residue mutated. For less potent agonists a differential effect was seen, which, it was believed, reflected the importance of the residues for ligand–protein interaction. These mutation studies were used to guide modeling of the heterocycles within the receptor. The *R*,*R* stereochemistry of each analogue was used in the modeling, based on previous studies,[12,14] and the protein models described previously[12,14] were used as starting points for this work. As with the earlier work, modeling was performed using the FLO+ computational software for docking (mcdock) and for energy minimizations (dockmin). Tethers were commonly used to explore potential H-bond interactions during docking procedures, and FLO interaction energy scores were used to identify satisfactory models.

The orientation of dexamethasone in relation to key residues in the active site of the receptor as determined from a crystal structure is shown (Figure 2A).[15] From previous studies,[14] the benzoxazinone of **7** and **8** (Table 5) acts as a hydrogen bond acceptor similar to the carbonyl of the steroidal A-ring (see ring A in **1–3**). Mutation studies confirm the relevance of both Arg611 and Gln570 for functional activity. However, the effect is compound-dependent (see discussions below). For dexamethasone, Arg611 was critical to activity (see Table 4) while Gln570 could be mutated with retention of activity. Close inspection of the crystal structure pose shows the direction of the H-bond from Gln570 to be much less favorable than Arg611; this may explain the dependency of dexamethasone on Arg611 and the insensitivity to Gln570. H-bonding interactions with these residues can be seen in the model shown for ethyl benzoxazinone **57D2E1** (Figure 2B) (structure shown in Table 5).[14] This is a refinement of the model previously described,[14] with an addition of a water molecule in the benzoxazinone region and reorientation of the two H-bonding residues, Arg611 and Gln570, to form favorable H-bonding interactions. The quinolone ring system was seen as a potential replacement for the benzoxazinone. Mutation results were not available for this heterocycle. However, modeling studies suggest that H-bonding to Gln570 is indeed possible but is unlikely to Arg611 (see Figure 2C for the *R*,*R* enantiomer of **18D1**) and that a water molecule is no longer favored in the A-ring region. For the indole, **20D1E1**, the mutation data indicate the importance of the Arg611 interaction despite the absence of an H-bond acceptor group in the molecule. An alternative interaction with Arg611 would be a cation–π interaction. Modeling suggests this

Table 3. Biological Data for N-Linked Quinoline/Isoquinoline Analogues

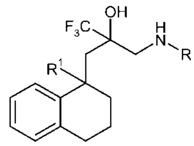

C'pound[a]	R	Stereo.	R^1	GR Binding[b,c] pIC_{50}	NFκB[b,d] pIC_{50} (% max)	MMTV[b,e] Agonism pEC_{50} (% max)	MMTV[b,f] Antagonism pIC_{50}
Dex **2**				8.10 ± 0.04	8.93 ± 0.07 (110% ± 5)	8.3 ± 0.23 (102% ± 10.8)	<5
Pred **3**				*nt*[g]	8.07 ± 0.15 (98.4% ± 3.8)	7.50 ± 0.49 (100.3% ± 0.15)	*nt*
4[h]				8.24 ± 0.09	< 6	*nt*	8.33 ± 0.36 (99.7% ± 0.49)
43D1	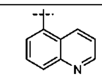	D1	Et	7.95 ± 0.15	7.91 ± 0.04 (64.5% ± 1.3)	< 6 (5.5% ± 0.6)	*nt*
45D1	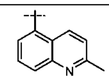	D1	Et	7.83 ± 0.19	8.62 ± 0.25 (90.7% ± 8.1)	7.88 ± 0.05 (73.2% ± 0.67)	*nt*
45D1E1	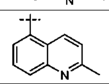	D1E1	Et	7.83 ± 0.17	8.71 ± 0.10 (97.7% ± 2.5)	7.96 ± 0.17 (62.1% ± 12.4)	*nt*
45D2	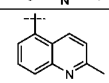	D2	Et	7.73 ± 0.12	7.31 ± 0.12 (66.6% ± 5.4)	6.79 ± 0.08 (42.5% ± 7.6)	*nt*
45D2E1	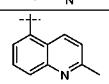	D2E1	Et	7.76 ± 0.14	7.34 ± 0.23 (65.9% ± 9.6)	6.54 ± 0.06 (19.5% ± 3.1)	*nt*
49D1	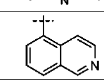	D1	Et	7.67 ± 0.04	8.90 ± 0.29 (87.9% ± 3.5)	7.49 ± 0.14 (19.1% ± 1.3)	*nt*
49D1E2	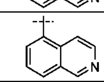	D1E2	Et	8.00 ± 0.16	8.66 ± 0.22 (89.8% ± 4.3)	< 6 (6.3% ± 4.3)	*nt*
54D1E2	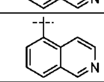	D1E2	Me	8.06 ± 0.24	8.93 ± 0.32 (80.8% ± 11.3)	8.08 ± 0.43 (28.9% ± 11.7)	6.99 ± 0.09 (69.2% ± 1.9)
54D2E1	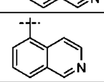	D2E1	Me	7.13 ± 0.14	7.82 ± 0.14 (91.6% ± 51)	6.59 ± 0.19 (26.7% ± 7.6)	*nt*
55D1E1	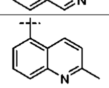	D1E1	Me	8.30 ± 0.23	9.30 ± 0.39 (101.4% ± 8.5)	8.02 ± 0.12 (47.6% ± 15.8)	7.11 ± 0.14 (37.2% ± 4.8)
55D2E1	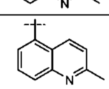	D2E1	Me	8.04 ± 0.11	8.04 ± 0.03 (93.7% ± 1.7)	7.14 ± 0.05 (60.5% ± 24.6)	*nt*
56D1E1	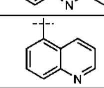	D1E1	Me	8.20 ± 0.19	8.51 ± 0.20 (68.7% ± 8.3)	7.87 ± 0.11 (20.0% ± 5.2)	*nt*

[a] D = diastereomer, E = enantiomer. The stereochemistry of the diastereomers has been consistently assigned by retention time on LC/MS. Enantiomer assignment is based on the order of elution from analytical chiral HPLC. See text for further details. [b] pIC_{50} values are from duplicate wells with at least $n = 3$ from 11-point dose–response curves with a top concentration of 10 mM. Standard errors are shown. [c] In the GR binding assay, compounds were tested for their ability to bind to GR using competition experiments with fluorescent labeled dexamethasone. [d] The NF*κ*B assay used human A549 lung epithelial cells engineered to contain a secreted placental alkaline phosphatase gene under the control of the distal region of the NF*κ*B dependent ELAM promoter. With a top concentration of 10 mM being tested, pIC_{50} values are not quoted for values less potent than $pIC_{50} = 6$. Maxima are quoted with reference to the maximum for dexamethasone (the standard used). [e] The MMTV transactivation assay human A549 lung epithelial cells were engineered to contain a renialla luciferase gene under the control of the distal region of the LTR from the mouse mammary tumor virus. [f] The GR antagonist assay used human A549 lung epithelial cells stably transfected with the mouse mammary tumor virus (MMTV) luciferase reporter gene. Compounds were tested for their ability to antagonize dexamethasone induced activation. [g] nt = not tested. [h] RU486 (mifepristone) was used as the standard for GR antagonism.

may be possible (see Figure 2D for **20D1E1**), but it would require movement of several side chains in the A-ring region and a repositioning of the tetrahydronapthalene left-hand side. Mutation studies with the C-linked quinolines (i.e., **33D1E1**) show a very interesting dependence on Arg611 and Glu570. These C-linked quinolines are shorter than other compounds studied and are capable of only taking one H-bond. An explanation for dependency on both residues, while having a diminished length, would be provided by the placing of a water molecule to act as a bridge (as seen in Figure 2E). However, despite the introduction of a water bridge, the C-linked quinolines appear to require a different positioning of the tetrahydronaphthalene group in the site, and this could explain the different SAR seen between the C-linked quinolines and the benzoxazinones at the tetrahydronaphthalene R^1 position, with functional activity being much reduced in the C-linked

Table 4. Effect of Mutations on the Activity in the NFκB Agonist Assay for Selected Compounds

compd	Q570A[a] (full NFκB agonism at 1 μM?)	R611A[a] (full NFκB agonism at 1 μM?)
dexamethasone	yes	no
fluticasone propionate	yes	yes
57D2E1	no	no
20D1E1	yes	no
33D1E1	no	no
45D1E1	yes	no

[a] The GR Q570A and GR R611A mutants were made in pcDNA3.1 by PCR using Quickchange mutagenesis kit from Strategene and pcDNA 3.1 wt GR as template. The mutants were then transfected into COS7 together with NFκB-luciferase reporter using Fugene reagent from Roche. The next day cells were treated with 10 ng/mL recombinant human TNFα in the absence or presence of 1 μM test compound. After overnight culture the luciferase activity was measured using Dual-Glo luciferase reagent from Promega and Invision plate reader. Q570A and R611A represent the mutations where glutamine 570 and arginine 611 have been mutated to alanine, respectively. The luciferase activity was compared with WT dexamethasone agonism. In this study full agonism was considered to be seen for a mutant if the luciferase response was equivalent to wild type. Absence of agonism was considered to be where the response was less than 20%.

quinolines on introduction of a cyclopentyl group (e.g., **40D1**), while the same change in the benzoxazinone series (e.g., **7**) leads to much enhanced functional activity.

Mutation studies with the N-linked quinolines **45D1E1** indicate a dependence on Arg611 alone. Modeling suggests that direct interaction with Arg611 can be achieved without water being present, but movement of the tetrahydronaphthalene portion of the molecule would be expected, with the tetrahydronaphthalene group occupying a position similar to that proposed for C-linked quinolines (Figure 2F). Interestingly, this again corresponds to a fall in functional activity on the introduction of the tetrahydronaphthalene R^1 cyclopentyl group (data not shown). No mutation data were available for the N-linked isoquinolines. However, modeling would suggest a weak interaction with Arg611 and Gln570. Reasonable electrostatic compatibility can be seen, but distances are rather long for an Arg611 H-bond interaction and the angle is acute for an H-bond to Gln570 (see Figure 2G).

Conclusion

This paper describes a series of tetrahydronaphthalene derivatives coupled to heterocycles that are potent glucocorticoid receptor partial agonists and full agonists having efficacy selectivity for transrepression over transactivation. Modeling studies show how these analogues may be binding into the active site of the receptor. The next challenge is to discover analogues with similar levels of selectivity that are also orally bioavailable to allow exploration of these molecular profiles in animal models.

Experimental Section

General Experimental Conditions. ^{1}H NMR. ^{1}H NMR spectra were recorded in either $CDCl_3$ or DMSO-d_6 on either a Bruker DPX 400 or Bruker Avance DRX spectrometer both working at 400 MHz and 9.4 T using as an internal standard of either tetramethylsilane or the residual protonated solvent. For $CDCl_3$ and DMSO-d_6 this was referenced to 7.25 and 2.50 ppm, respectively.

LCMS System A. This consisted of a Waters ZQ platform with a HP1050 autosampler. The column was a 3.3 cm × 4.6 mm, 3 μm ABZ+PLUS. The flow rate was 3 mL/min, and the injection volume was 5 μL. UV detection was in the range 215–330 nm. The mobile phase consisted of solvent A (0.1% formic acid plus 10 mM ammonium acetate) and solvent B (95% acetonitrile plus 0.05% formic acid) with a gradient of 100% solvent A for 0.7 min changing to 100% solvent B over 3.5 min, maintained for 1.1 min, then reverting to 100% solvent A over 0.2 min.

LCMS System B. System B consisted of a Finnigan TSQ700 platform with an electrospray source operating in positive or negative ion mode with a HP1050 autosampler. The column was a 100 mm × 3 mm, 5 μm Higgins Clipeus C18, and the flow rate was 2 mL/min. UV detection was at 254 nm. The mobile phase consisted of solvent A (water plus 0.1% formic acid) and solvent B (acetonitrile plus 0.1% formic acid) with a gradient of 95% solvent A for 1 min changing to 5% solvent A over 14 min, maintained for 2 min, then reverting to 95% solvent A over 1 min and maintained for 2 min. System A was used except where stated otherwise.

LCMS System C. This consisted of a Waters ZQ platform with a HP1050 autosampler. The column was a 3.3 cm × 4.6 mm, 3 μm ABZ+PLUS. The flow rate was 3 mL/min, and the injection volume was 5 μL. UV detection was in the range 215–330 nm. The mobile phase consisted of solvent A (0.1% formic acid plus 10 mM ammonium acetate) and solvent B (95% acetonitrile plus 0.05% formic acid) with a gradient of 100% solvent A for 0.7 min changing to 100% solvent B over 4.2 min, maintained for 1.1 min, then reverting to 100% solvent A over 0.2 min. System A was used except where stated otherwise.

Mass Directed Reverse-Phase HPLC Chromatography (System 1). This was carried out on a 10 cm × 21.3 mm, 5 μm Supelco column and with a flow rate of 20 mL/min. The injection volume was 500 μL, and the UV detection range was 200–320 nm. The mobile phase consisted of solvent A (water plus 0.1% formic acid) and solvent B (60% MeCN plus 0.05% formic acid) with a gradient of 40% solvent A for 1 min changing to 35% solvent A over 9 min and then changing to 1% solvent A over 3.5 min and maintained for 1.4 min before reverting to 40% solvent A over 0.1 min.

Reverse-Phase HPLC Chromatography (System 2). Preparative HPLC was carried out on a C18-reverse-phase column (250 mm × 21.2 mm id Supelco ABZ++ column with 5 μm particle size), eluting isocratically with 40% solvent A and 60% solvent B, where solvent A is water + 0.1% formic acid and solvent B is 95% aqueous MeCN + 0.05% formic acid.

Reverse-Phase HPLC Chromatography (System 3). Preparative HPLC was carried out on a C18-reverse-phase column (10 cm × 2.1 cm id Genesis column with 7 μm particle size), eluting with a gradient of acetonitrile (containing 0.1% trifluoroacetic acid) and water (containing 0.1% trifluoroacetic acid) at a flow rate of 5 mL/min. UV detection at 230 nm was used unless otherwise stated.

Reverse-Phase HPLC Chromatography (System 4). Preparative HPLC was carried out on a C18-reverse-phase column (10 cm × 21.2 mm id Supelcosil LCABZ+Plus column with 5 μm particle size), eluting with a solvent gradient of 40/60% solvent A/B to 15%/85% A/B. Solvent A was water containing 0.1% formic acid, and solvent B was 95% MeCN and 5% water containing 0.05% formic acid.

1-{3,3,3-Trifluoro-2-hydroxy-2-[(1-methyl-1,2,3,4-tetrahydro-1-naphthalenyl)methyl]propyl}-4(1*H*)-quinolinone 17D1 and 17D2. To the epoxide **16D1** (0.05 g, 0.19mmol), 4-hydroxyquinoline (0.027 g, 0.19mmol), and dimethylformamide (0.4 mL) was added potassium *tert*-butoxide (0.020 g, 0.19mmol), and the reaction vessel was stoppered for 3 h at room temperature. The crude material was purified by mass directed reverse-phase HPLC (system 1) to afford the **17D1** (racemic diastereomer 1) (0.06 g, 8%). LCMS: t_R = 3.42 min; MH^+ = 416. ^{1}H NMR: δ_H ($CDCl_3$, 400 MHz) 8.32 (dd, 1H), 7.49 (m, 1H), 7.43–7.36 (m, 2H), 7.30 (m, 1H), 7.23–7.12 (m, 4H), 7.03 (d, 1H), 6.16 (d, 1H), 4.17 (d, 1H), 3.89 (d, 1H), 2.88–2.75 (m, 2H), 2.64–2.56 (m, 2H), 2.49 (d, 1H), 2.25 (d, 1H), 2.00–1.92 (m, 1H), 1.87–1.73 (m, 2H), 1.36 (s, 3H). **17D1** $C_{24}H_{25}F_3NO_2$ (MH^+): calcd 416.1837, found 416.1847.

17D2 (racemic diastereomer 2) was similarly prepared from **16D2**. LCMS: t_R = 3.43 min; MH^+ = 416. ^{1}H NMR: δ_H ($CDCl_3$, 400 MHz) 8.44 (dd, 1H), 7.63 (m, 2H). 7.44 (d, 1H), 7.38–7.35

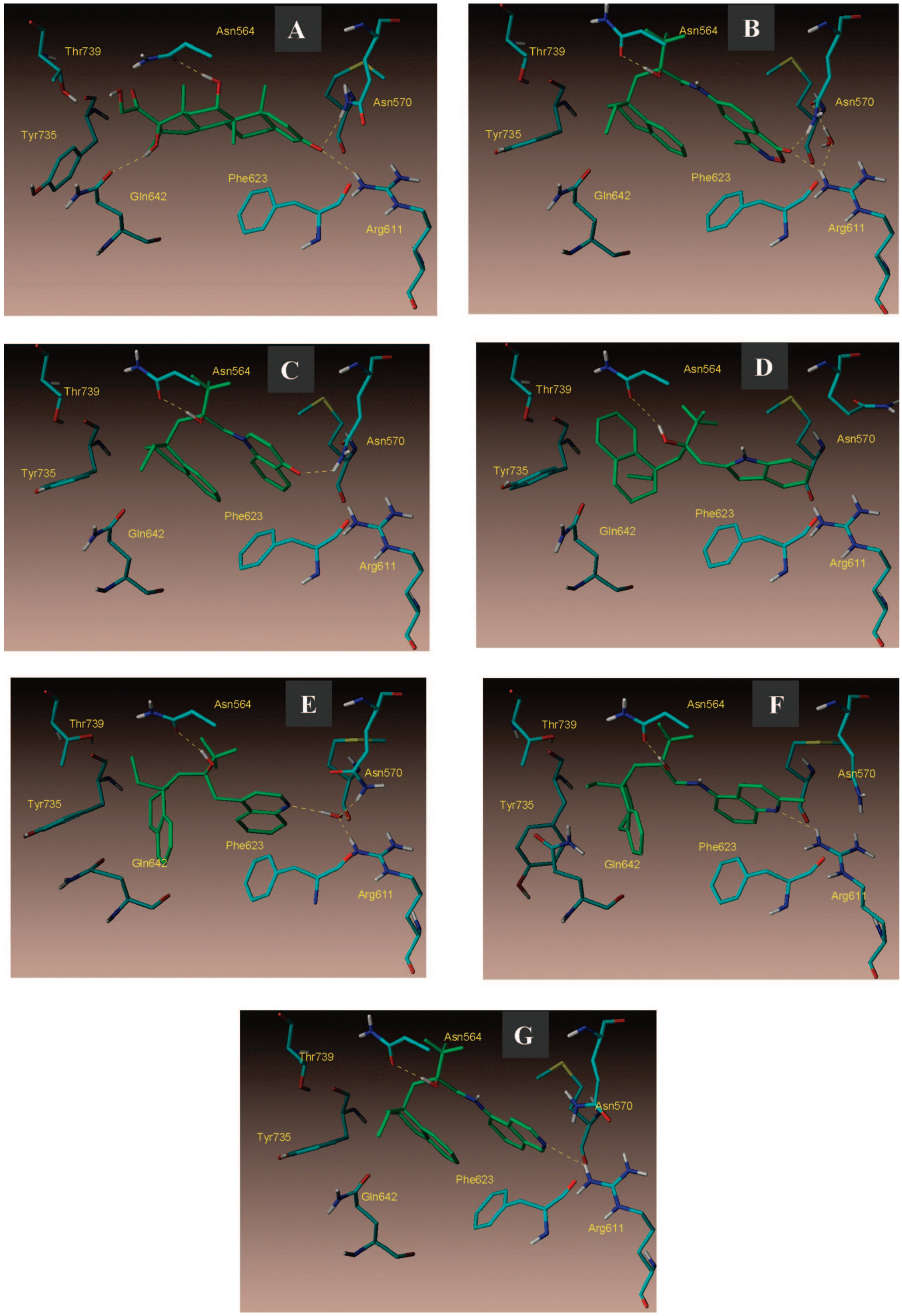

Figure 2. All the ligands are shown in green with key residues from the active site of the glucocorticoid receptor shown in cyan. All nonsteroidal analogues are modeled with the *R*,*R* stereochemistry based on previous studies.[14] H-bonding interactions are shown as dotted lines. The active site is viewed from the same perspective in each part. (A) Dexamethasone as found in the crystal structure[15] with the ketone of the A-ring forming H-bonds to Asn570 and Arg611. (B) Modeling of the benzoxazine **57D2E1**, showing refinements to the benzoxazine H-bonding region with a water molecule included and the Arg611 and Gln570 positions modified from those used in previous studies.[14] (C) Modeling of the quinolone analogue **18D1**. Note the absence of the water molecule and that the tetrahydronaphthalene is oriented similarly to **7** in part B. (D) Modeling of the indole analogue **20D1E1**. Note the different orientation of the tetrahydronaphthalene compared with part B or C. (E) Modeling of the C-linked quinoline analogue **33D1E1**. Note a further different orientation of the tetrahydronaphthalene and the water molecule bridging the quinoline nitrogen and Asn570 and Arg611. (F) Modeling of the N-linked quinoline analogue **45D1E1**. The tetrahydronaphthalene is oriented similarly to the C-linked quinoline (see part E), but the bridging water is not required with **45D1E1** compared with **33D1E1**. (G) Modeling of the N-linked isoquinoline analogue **49D1E2** in an orientation similar to that of **45D1E1** in part F.

(m, 3H), 7.25–7.08 (m, 3H), 6.30 (d, 1H), 4.41 (dd, 2H), 2.80–2.67 (m, 3 h), 2.45 (bs, 1H), 2.24–1.95 (m, 2H), 1.82–1.67 (m, 2H), 1.43–1.34 (m, 1H), 1.30 (s, 3H). **17D2** $C_{24}H_{25}F_3NO_2$ (MH^+): calcd 416.1837, found 416.1852.

Table 5. Biological Data for R^1 = Et and Cyclopentyl Analogues of Tetrahydronaphthalene–Benzoxazinones

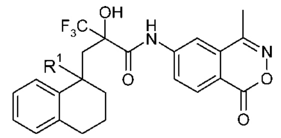

compd[a]	R^1	GR binding,[b,c] pIC_{50}	NFκB[b,d] pIC_{50} (% max)	MMTV[b,e] agonism, pEC_{50} (% max)	MMTV[b,f] antagonism, pIC_{50}
7D2E2	pentyl[c]	8.09±0.35	8.69±0.45(92%±22)	7.75±0.58(39%±9)	7.27±0.6
57D2E1	Et	8.21±0.21	8.3 ±0.43(73%±11)	8.04±0.14(31%±9)	6.7 ±0.44

[a] D = diastereomer, E = enantiomer. The stereochemistry of the diastereomers has been consistently assigned by retention time on LC/MS. Enantiomer assignment is based on the order of elution from analytical chiral HPLC. See text for further details. [b] pIC_{50} values are from duplicate wells with at least n = 3 from 11-point dose–response curves with a top concentration of 10 mM. Standard errors are shown. [c] In the GR binding assay, compounds were tested for their ability to bind to GR using competition experiments with fluorescent labeled dexamethasone. [d] The NFκB assay used human A549 lung epithelial cells engineered to contain a secreted placental alkaline phosphatase gene under the control of the distal region of the NFκB dependent ELAM promoter. With a top concentration of 10 mM being tested, pIC_{50} values are not quoted for values less potent than pIC_{50} = 6. Maxima are quoted with reference to the maximum for dexamethasone (the standard used). [e] The MMTV transactivation assay human A549 lung epithelial cells were engineered to contain a renialla luciferase gene under the control of the distal region of the LTR from the mouse mammary tumor virus. [f] The GR antagonist assay used human A549 lung epithelial cells stably transfected with the mouse mammary tumor virus (MMTV) luciferase reporter gene. Compounds were tested for their ability to antagonize dexamethasone induced activation.

3-(1-Methyl-1,2,3,4-tetrahydro-1-naphthalenyl)-1,1,1-trifluoro-2-(1*H*-indol-2-ylmethyl)-2-propanol 19D1 and 19D2. A solution of *n*-butyllithium (1.6 M in hexanes, 3.9 mL, 6.24mmol) was added dropwise to a stirred solution of 2-methylindole (0.273 g, 2.08 mmol) in dry THF (7.5 mL) at −70 °C under nitrogen. After 5 min, a solution of potassium *tert*-butoxide (4.2 mL, 4.2 mmol, 1 M in THF) was added dropwise. The mixture was then warmed to −30 to −25 °C and stirred for 10 min, giving a bright-yellow precipitate. After the mixture was recooled to −70 °C, the trifluoromethyl ketone **14** (0.523 g, 2.08 mmol) in dry THF (2.5 mL) was added. After ~1 h, the reaction was quenched with water (50 mL) and the sample was extracted with EtOAc (50 mL). The organic phase was washed with brine and dried ($MgSO_4$). Solvent removal in vacuo followed by purification on silica (50 g), eluting with a 0–50% gradient of dichloromethane in cyclohexane, gave the title compound as a yellow oil (0.179 g, 23%). Subsequent preparative reverse-phase HPLC (system 2) of a small sample gave diastereomer 1 **19D1** (t_R = 31.13 min) and diastereomer 2 **19D2** (t_R = 32.77 min).

19D1. LCMS: t_R = 3.09 min; MH+ = 388. ^{1}H NMR: δ_H ($CDCl_3$, 400 MHz) 7.94 (bs, 1H), 7.57 (d, 1H), 7.17 (t, 1H), 7.12 (t, 1H), 7.06–6.98 (m, 2H), 6.90 (d, 1H), 6.69 (t, 1H), 6.30 (s, 1H), 3.55 (bs, 1H), 2.2.93–2.80 (m, 2H), 2.80–2.67 (m, 2H), 2.58 (d, 1H), 2.46–2.37 (m, 1H), 2.34 (s, 1H), 2.14 (d, 1H), 1.92–1.62 (m, 3H), 1.26 (s, 3H). **19D1** $C_{22}H_{25}F_3NO$ (MH^+): calcd 388.1888, found 388.1898.

19D2. LCMS: t_R = 3.09 min; MH+ = 388. ^{1}H NMR: δ_H ($CDCl_3$, 400 MHz) 8.29 (bs, 1H), 7.55 (d, 1H), 7.42 (d, 1H), 7.28 (m, 1H), 7.23 (t, 1H), 7.19–7.11 (m, 2H), 7.07 (t, 1H), 6.32 (s, 1H), 3.54 (bs, 1H), 3.32 (d, 1H), 3.17 (d, 1H), 2.85–2.72 (m, 1H), 2.64 (d, 1H), 2.22 (s, 1H), 2.17–2.08 (m, 1H), 2.02 (m, 2H), 1.83–1.74 (m, 2H), 1.34 (s, 3H).

3-(1-Ethyl-1,2,3,4-tetrahydro-1-naphthalenyl)-1,1,1-trifluoro-2-(1*H*-indol-2-ylmethyl)-2-propanol 20D1, 20D1E1, 20D1E2. A solution of 2-methylindole (97 mg, 0.74 mmol) in anhydrous diethyl ether (15 mL) was treated with *n*-butyllithium (1.4 mL of a 1.6 M solution in hexanes, 2.22 mmol). Potassium *tert*-butoxide (149 mg, 1.33 mmol) was added, and the mixture was stirred at room temperature for 10 min to give an orange solution. A solution of **13** (200 mg, 0.74 mmol) in diethyl ether (2 mL) was added dropwise, and the mixture was stirred for 30 min to give a red solution. The mixture was partitioned between ethyl acetate (20 mL) and water (20 mL), and the organic phase was separated, dried ($MgSO_4$), and evaporated. The residue was purified by flash chromatography (silica, pentane/diethyl ether, 9:1, as eluent) and then by HPLC (system 3) to give a mixture of the diastereomers of the title compound (70 mg) as a light-brown oil. LCMS (system B): t_R = 14.86 and 14.97 min; MH^+ = 402. Subsequent HPLC (system 2) purification of the mixture of diastereomers gave diastereomer 1 **20D1** (t_R = 34.56 min) and diastereomer 2 **20D2** (t_R = 36.76 min).

20D1. LCMS (system C): t_R = 4.06 min; MH^+ = 402, MH^- = 400. ^{1}H NMR: δ_H ($CDCl_3$, 400 MHz) 7.92 (s, 1H), 7.58 (d, 1H), 7.25 (d, 1H), 7.20–6.98 (m, 4H), 6.82 (d, 1H), 6.63 (t, 1H), 6.30 (s, 1H), 2.92–2.65 (m, 4H), 2.45 (d, 1H), 2.22 (m, 2H), 1.88 (m, 2H), 1.73 (m, 2H), 1.55 (m, 2H), 0.80 (t, 3H). **20D1** $C_{24}H_{27}F_3NO$ (MH^+): calcd 402.2045, found, 402.2057.

20D2. LCMS (system C): t_R = 4.08 min; MH^+ = 402, MH^- = 400. ^{1}H NMR: δ_H ($CDCl_3$, 400 MHz) 8.37 (s, 1H), 7.55 (d, 1H), 7.39 (d, 1H), 7.30–7.03 (m, 6H), 6.31 (s, 1H), 3.32 (d, 1H), 3.18 (d, 1H), 2.80 (m, 2H), 2.53 (d, 1H), 2.03 (m, 3H), 1.85–1.45 (m, 5H + excess), 0.83 (t, 3H).

20D1 (20 mg) was further separated into its enantiomers using a 2 cm × 25 cm Chiralcel OD column, eluting with 5% EtOH in heptane with a flow rate of 15 mL/min. Diastereomer 1, enantiomer 1 **20D1E1** eluted around 12.1 min (4.1 mg), and diastereomer 1, enantiomer 2 **20D1E2** eluted around 16.4 min (4.1 mg).

20D1E1. Analytical chiral HPLC (25 cm × 0.46 cm Chiralcel OD column, 5% EtOH in heptane, eluting at 1 mL/min): t_R = 9.4 min. LCMS (system C): t_R = 4.11 min; MH^+ = 402, MH^- = 400. **20D1E1** $C_{24}H_{27}F_3NO$ (MH^+): calcd 402.2045, found 402.2054.

20D1E2. Analytical chiral HPLC (25 cm × 0.46 cm Chiralcel OD column, 5% EtOH in heptane, eluting at 1 mL/min): t_R = 12.2 min. LCMS (system C): t_R = 4.11 min; MH^+ = 402, MH^- = 400. **20D1E2** $C_{24}H_{27}F_3NO$ (MH^+): calcd 402.2045, found 402.2060

2-{2-[(1-Ethyl-1,2,3,4-tetrahydro-1-naphthalenyl)methyl]-3,3,3-trifluoro-2-hydroxypropyl}-4-methyl-1*H*-indole-6-carbonitrile 21D1, 21D1E1, 21D1E2. A mixture of **28D1** (50 mg, 0.16 mmol), **27** (57 mg, 0.23 mmol), copper(I) iodide (4.6 mg, 0.024 mmol), and tetramethylguanidine (0.12 mL, 0.97 mmol) in 1,4-dioxane (0.4 mL) was degassed and flushed with N_2 six times. Bis(triphenylphosphine)palladium chloride (11.3 mg, 0.016mmol) was added, and the mixture was degassed and flushed with N_2 six times. The mixture was stirred at 80 °C for 18 h. After this time the mixture was allowed to cool and then filtered through Celite, poured into DCM (30 mL), washed with 1 M sulfuric acid (3 × 20 mL), water (3 × 20 mL), and brine (20 mL), dried ($MgSO_4$), and reduced under vacuum. The residue was diluted with methanol (5 mL), treated with sodium hydroxide (100 mg), and stirred at 50 °C, for 1 h. The mixture was concentrated under vacuum, diluted with DCM (30 mL), and washed with brine (30 mL). The organic layer was dried ($MgSO_4$) and reduced under vacuum. The crude material was purified by HPLC (system 4) to afford diastereomer 1 **21D1**, a single diastereomer of the title compound (3.2 mg). (Note that the nomenclature for this diastereomer is based on the use of a single diastereomer of starting material **28D1**.) LCMS (system C): t_R = 4.15 min; MH^+ = 441. ^{1}H NMR: δ_H ($CDCl_3$, 400 MHz) 8.34 (s, 1H), 7.43 (s, 1H), 7.13 (s, 1H), 7.11–7.03 (m, 2H), 6.83 (d, 1H), 6.72 (m, 1H), 6.31 (s, 1H), 2.95–2.84 (m, 2H), 2.83–2.66 (m, 3H), 2.52 (s, 3H), 2.44 (d, 1H), 2.35 (m, 1H), 2.25–2.15 (m, 2H), 1.90–1.48 (m, >5H), 0.80 (t, 3H). **21D1** $C_{26}H_{28}F_3N_2O$ (MH^+): calcd 441.2154, found 441.2171. **21D1** was further separated into its enantiomers using a 2 cm × 25 cm Chiralpak AD column, eluting with 8% ^{i}PrOH in heptane with a flow rate of 15 mL/min. Diastereomer 1, enantiomer 1 **21D1E1** eluted around 11.1 min, and diastereomer 1, enantiomer 2 **21D1E2** eluted around 13.5 min.

21D1E1. Analytical chiral HPLC (25 cm × 0.46 cm Chiralpak AD column, 8% ^{i}PrOH in heptane, eluting at 1 mL/min): t_R = 7.8 min. LCMS (system C): t_R = 4.15 min; MH^+ = 441.

21D1E2. Analytical chiral HPLC (25 cm × 0.46 cm Chiralpak AD column, 8% ^{i}PrOH in heptane, eluting at 1 mL/min): t_R = 10.7 min. LCMS (system C): t_R = 4.15 min; MH^+ = 441. **21D1E2** $C_{26}H_{28}F_3N_2O$ (MH^+): calcd 441.2154, found 441.2170.

2-{2-[(1-Ethyl-1,2,3,4-tetrahydro-1-naphthalenyl)methyl]-3,3,3-trifluoro-2-hydroxypropyl}-1*H*-indole-3-carbonitrile 22D1, 22D1E1, 22D1E2. The indole **20D1** (0.20 g, 0.47mmol) was dissolved in dry acetonitrile (15 mL) and cooled under nitrogen to 5 °C. Chlorosulfonyl isocyanate (0.043 mL) in acetonitrile (1.5 mL) was added slowly, and the mixture was stirred for 30 min. Dimethylformamide (0.042 mL) was then added, and the mixture was allowed to warm to room temperature over 2 h. The mixture was poured into water and extracted with dichloromethane (2 × 10 mL). The organic layer was washed with brine (10 mL), dried ($MgSO_4$), and concentrated in vacuo. The residue was purified by HPLC (system 3) using a 50–95% acetonitrile gradient to afford the title compound (0.005 g, 2%) as a gray solid. LCMS (system C): t_R = 3.85min; MH^+ = 427, MNH_4^+ = 444, MH^- = 425. ^{1}H NMR: δ_H ($CDCl_3$, 400 MHz) 8.69 (bs, 1H), 7.72 (s, 1H), 7.33–7.25 (m, >4H), 7.07 (d, 1H), 7.01 (t, 1H), 6.72 (d, 1H), 6.55 (t, 1H), 3.07 (q, 2H), 2.85–2.67 (m, 2H), 2.47–2.42 (m, 2H), 2.28–2.11 (m, 2H), 1.93–1.63 (m, 8H), 0.81 (t, 3H).

This diastereomer **22D1** was further separated into its enantiomers using a 2 cm × 25 cm Chiralpak AS column, eluting with 5% EtOH in heptane with a flow rate of 15 mL/min. Diastereomer 1, enantiomer 1 **22D1E1** eluted around 11.5 min, and diastereomer 1, enantiomer 2 **22D1E2** eluted around 14.5 min.

22D1E1. Analytical chiral HPLC (25 cm × 0.46 cm Chiralpak AS column, 5% EtOH in heptane, eluting at 1 mL/min): t_R = 8.96 min. LCMS (system C): t_R = 3.85min; MH^+ = 427, MNH_4^+ = 444, MH^- = 425. **22D1E1** $C_{25}H_{26}F_3N_2O$ (MH^+): calcd 427.1997, found 427.2011.

22D1E2. Analytical chiral HPLC (25 cm × 0.46 cm Chiralpak AS column, 5% EtOH in heptane, eluting at 1 mL/min): t_R = 11.31 min. LCMS (system C): t_R = 3.85min; MH^+ = 427, MNH_4^+ = 444, MH^- = 425.

3-(1-Ethyl-1,2,3,4-tetrahydro-1-naphthalenyl)-1,1,1-trifluoro-2-(1*H*-pyrrolo[2,3-*c*]pyridin-2-ylmethyl)-2-propanol 23D1, 23D1E1, 23D1E2. A mixture of **28D1** (50 mg, 0.161 mmol), **31** (51 mg, 0.193 mmol), copper(I) iodide (4.6 mg, 0.024 mmol), and 1,1,3,3-tetramethylguanidine (0.121 mL, 0.967 mmol) in 1,4-dioxane (0.4 mL) was degassed by evacuation and flushing with nitrogen six times. Dichlorobis(triphenylphosphine)palladium(II) (11.3 mg, 0.016 mmol) was added, and the resultant was degassed by evacuation and flushing with nitrogen a further six times. The mixture was heated at 80 °C for 18 h, then cooled, diluted with dichloromethane (40 mL), and washed with water (3 × 20 mL). The organic extracts were dried ($MgSO_4$) and concentrated in vacuo to give a crude reaction product (80 mg). This sample was diluted with methanol (5 mL), treated with sodium hydroxide (100 mg), and heated at reflux for 1.5 h. After cooling, it was diluted with dichloromethane (30 mL) and washed with brine (15 mL). The organic phase was dried ($MgSO_4$) and concentrated in vacuo and then purified using a 5 g silica SPE cartridge. Elution with successive mixtures of dichloromethane/methanol/triethylamine (99.5:0:0.5, 98.5:1:0.5, 97.5:2:0.5, 96.5:3:0.5, and then 95.5:4:0.5) gave 30 mg of product. Further purification using a preparative TLC plate, eluting with dichloromethane/methanol/triethylamine (89.5:10:0.5), gave 10 mg of product. Yet further purification using a 1 g aminopropyl SPE cartridge, eluting with dichloromethane and then dichloromethane.methanol (95:5), gave the title compound, a single diastereomer of the compound **23D1** (5.6 mg, 9%). LCMS (system C): t_R = 2.90 min; MH^+ = 403. ^{1}H NMR: δ_H ($CDCl_3$, 400 MHz) 8.63 (s, 1H), 8.19 (d, 1H), 7.46 (d, 1H), 7.05 (m, 2H), 6.90 (d, 1H), 6.78 (m, 1H), 6.25 (s, 1H), 2.97–2.67(m, 5H), 2.47 (d, 1H), 2.35–2.17(m, 2H), 1.94–1.66(m, 4H), 1.54 (m, 1H), 1.29 (m, 1H), 0.79 (t, 3H). **23D1** $C_{23}H_{26}F_3N_2O$ (MH^+): calcd 403.1997, found 403.2010. This diastereomer **23D1** was further separated into its enantiomers using a 2 cm × 25 cm Chiralcel OJ column, eluting with 15% EtOH in heptane with a flow rate of 15 mL/min. Diastereomer 1, enantiomer 1 **23D1E1** eluted around 5.0 min, and diastereomer 1, enantiomer 2 **23D1E2** eluted around 7.8 min.

23D1E1. Analytical chiral HPLC (25 cm × 0.46 cm Chiralcel OJ column, 15% EtOH in heptane, eluting at 1 mL/min): t_R = 4.25 min. LCMS (system C): t_R = 2.90 min; MH^+ = 403. **23D1E1** $C_{23}H_{26}F_3N_2O$ (MH^+): calcd 403.1997, found 403.2013.

23D1E2. Analytical chiral HPLC (25 cm × 0.46 cm Chiralcel OJ column, 15% EtOH in heptane, eluting at 1 mL/min): t_R = 7.53 min. LCMS (system C): t_R = 2.90 min; MH^+ = 403.

3-(1-Ethyl-1,2,3,4-tetrahydro-1-naphthalenyl)-1,1,1-trifluoro-2-(4-quinolinylmethyl)-2-propanol 33D1, 33D2, 33D1E1, 33D1E2. A solution of diisopropylamine (100 mg, 1.0 mmol) in dry tetrahydrofuran (5 mL) under a nitrogen atmosphere was cooled to −10 °C and treated with *n*-butyllithium (0.625 mL of a 1.6 M solution in hexanes, 1.0 mmol). The mixture was cooled to −78 °C and treated with a solution of 4-methylquinoline **32** (116 mg, 0.815 mmol) in dry tetrahydrofuran (1 mL), which gave an orange precipitate after 10 min. A solution of **13** (200 mg, 0.741 mmol) in dry tetrahydrofuran (1 mL) was added, giving a red solution that turned green after 10 min. The mixture was allowed to warm to −10 °C and was partitioned between ethyl acetate (40 mL) and water (40 mL). The organic phase was separated, dried ($MgSO_4$), and evaporated to give a yellow solid. The solid was recrystallized from ethyl acetate/cyclohexane to give **33D1** (diastereomer 1, 165 mg) as a white solid. The liquors from the recrystallization were purified by flash chromatography (silica, dichloromethane/ethyl acetate, 4:1, as eluent) and trituration with pentane to give **33D2** (diastereomer 2, 8 mg) as a white solid.

Racemic Diastereomer 1 33D1. LCMS (system B): t_R = 6.70 min; MH^+ = 414. ^{1}H NMR: δ_H ($CDCl_3$, 400 MHz) 8.75 (d, 1H), 8.18 (d, 1H), 7.78 (d, 1H), 7.73 (t, 1H), 7.54 (t, 1H), 7.22 (d, 1H), 7.09–6.92 (m, 4H), 3.21 (d, 1H), 3.04 (d, 1H), 2.88–2.71 (m, 2H), 2.46–2.36 (m, 2H), 2.30 (d, 1H), 1.97–1.50 (m, 6H), 0.83 (t, 3H). **33D1** $C_{25}H_{27}F_3NO$ (MH^+): calcd 414.2045, found 414.2042.

Racemic Diastereomer 2 33D2. LCMS (system B): t_R = 7.27 min; MH^+ = 414. ^{1}H NMR: δ_H ($CDCl_3$, 400 MHz) 8.82 (d, 1H), 8.11 (d, 1H), 8.00 (d, 1H), 7.70 (t, 1H), 7.55 (t, 1H), 7.37 (m, 2H), 7.23–6.97 (m, 4H), 3.50 (s, 2H), 2.73 (m, 2H), 2.59 (d, 1H), 2.15 (d, 1H), 2.08 (s, 1H), 1.93–1.83 (m, 2H), 1.78–1.48 (m, >6H), 0.78 (t, 3H). **33D2** $C_{25}H_{27}F_3NO$ (MH^+): calcd 414.2045, found 414.2058.

Diasteromer 1 **33D1** was separated into its enantiomers using a 2 cm × 25 cm Chiralcel OJ column, eluting with 5% EtOH in heptane with a flow rate of 15 mL/min. Enantiomer 1 **33D1E1** eluted around 10.7 min, and enantiomer 2 **33D1E2** eluted around 13.1 min.

33D1E1. Analytical chiral HPLC (25 cm × 0.46 cm Chiralcel OJ column, 5% EtOH in heptane, eluting at 1 mL/min): t_R = 8.90 min. LCMS (system C): t_R = 3.74 min; MH^+ = 414. **33D1E1** $C_{25}H_{27}F_3NO$ (MH^+): calcd 414.2045, found 414.2055.

33D1E2. Analytical chiral HPLC (25 cm × 0.46 cm Chiralcel OJ column, 5% EtOH in heptane, eluting at 1 mL/min): t_R = 11.44 min. LCMS (system C): t_R = 3.74 min; MH^+ = 414.

3-(1-Ethyl-1,2,3,4-tetrahydro-1-naphthalenyl)-1,1,1-trifluoro-2-{[(2-methyl-5-quinolinyl) amino]methyl}-2-propanol 45D1, 45D1E1, 45D1E2. A solution of **15D1** (racemic diastereomer 1, 83 mg, 0.29mmol) in dry dimethylacetamide (1 mL) was added to a mixture of 2-methyl-5-quinolinamine **44** (55 mg, 0.35mmol) and potassium *tert*-butoxide (39 mg, 0.35mmol) in dry dimethylacetamide (1 mL) under a nitrogen atmosphere. The mixture was stirred at room temperature for 2 h. The mixture was then poured into brine/water (1:1) and extracted with ethyl acetate. The organic extracts were washed further with brine/water (1:1), passed through a hydrophobic frit, and evaporated in vacuo to yield a brown oil. The crude product was applied first to a 5 g of silica SPE cartridge, eluting with 0 to 15% ethyl acetate in cyclohexane gradient and then to a 2g silica SPE cartridge eluting with 0–15% diethylether in cyclohexane gradient to give the title compound **45D1** (racemic diastereomer 1) (8 mg). LCMS: $t_R = 3.07$ min; $MH^+ = 443$. ^1H NMR: δ_H ($CDCl_3$, 400 MHz) 7.95 (d, 1H), 7.47 (d, 1H), 7.38 (d, 1H), 7.36–7.31 (m, 2H), 7.24–7.17 (m, 4H), 5.93 (d, 1H), 4,10 (bd, 1H), 3.32–3.23 (m, 1H), 2.90 (dd, 1H), 2.84–2.74 (m, 2H), 2.72 (s, 3H), 2.37–2.22 (m, 3H), 1.92–1.58 (m, 5H), 0.86 (t, 3H). **45D1** $C_{26}H_{30}F_3N_2O$ (MH^+): calcd 443.2310, found 443.2317.

Racemic diastereomer 1 **45D1** was separated into its enantiomers using a 2 cm × 25 cm Chiralcel OJ column, eluting with 15% ethanol in heptane with a flow rate of 15 mL/min to yield diastereomer 1 enantiomer 1 **45D1E1** eluting around 6 min and diastereomer 1 enantiomer 2 **45D1E2** eluting around 9 min.

45D1E1. Analytical chiral HPLC (25 cm × 0.46 cm Chiralcel OJ column, 15% ethanol in heptane, eluting at 1 mL/min): $t_R = 4.77$ min. This enantiomer was further purified by application to a 2 g silica SPE cartridge, eluting with heptane followed by 0–25% diethyl ether in cyclohexane gradient. LCMS: $t_R = 3.07$ min; $MH^+ = 443$. ^{19}F NMR: δ ($CDCl_3$) −80.37. **45D1E1** $C_{26}H_{30}F_3N_2O$ (MH^+): calcd 443.2310, found 443.2314.

45D1E2. Analytical chiral HPLC (25 cm × 0.46 cm Chiralcel OJ column, 15% ethanol in heptane, eluting at 1 mL/min): $t_R = 7.83$ min. LCMS: $t_R = 3.07$ min; $MH^+ = 443$. ^{19}F NMR: δ ($CDCl_3$) −80.38.

2-[(1-Ethyl-1,2,3,4-tetrahydro-1-naphthalenyl)methyl]-3,3,3-trifluoro-2-hydroxypropanal 47D1+D2. To a solution of 2-[(1-ethyl-1,2,3,4-tetrahydro-1-naphthalenyl)methyl]-3,3,3-trifluoro-1,2-propanediol **46D1+D2** (2.03 g, 6.71mmol) (prepared as for **52D1+D2**; see below) in anhydrous dichloromethane (50 mL), anhydrous dimethyl sulfoxide (50 mL), and triethylamine (5.9 mL, 42mmol) stirred under nitrogen in an ice–water bath at 9 °C was added a pyridine–sulfur trioxide complex (5.37 g, 33mmol) portionwise over 20 min. The solution was then allowed to warm to room temperature and stirred for 65 h. The reaction mixture was added to aqueous ammonium chloride solution (350 mL) and extracted into dichloromethane (×2). The combined organic layers were washed successively with water (2 × 200 mL) and saturated brine (2 × 200 mL), dried over anhydrous magnesium sulfate, and evaporated in vacuo. The brown oil obtained was applied to a 50 g silica SPE cartridge, eluting with 0–100% dichloromethane in heptane gradient to give the title compound as a 40:60 mixture of diastereomers (380 mg, 19%). LCMS: $t_R = 3.64$ min; $M + NH_4^+ = 318$. ^1H NMR: δ_H ($CDCl_3$) 9.60 (s, 0.6H), 8.82 (s, 0.4H), 7.36–7.27 (m, 1H), 7.20–7.05 (m, 3H), 3.81 (0.4H), 3.37 (s, 0.6H), 2.93–2.45 (m, 3H), 2.32 (d, 0.4H), 2.16–2.07 (m, 0.6H), 1.95–1.73 (m, 5H), 1.72–1.52 (m, 1H), 1.37 (s, 0.4 × 3H), 0.84 (t, 3H). ^{19}F NMR: δ ($CDCl_3$) −77.9 and −78.3 (40:60 ratio of diastereomers).

3-(1-Ethyl-1,2,3,4-tetrahydro-1-naphthalenyl)-1,1,1-trifluoro-2-[(5-isoquinolinylamino)methyl]-2-propanol 49D1, 49D2, 49D1E1, 49D1E2. A solution of aldehyde **47D1+D2** (220 mg, 0.73mmol) and 5-isoquinolinamine **48** (144 mg, 1.0mmol) in glacial acetic acid (4 mL) was microwaved at 150 °C for 20 min. The solution was added to toluene and evaporated in vacuo to yield an orange residue. The crude product was purified on a 10 g silica SPE cartridge, eluting with 0–100% dichloromethane in heptane gradient to give the imine as a mixture of diastereomers (190 mg, 61%). LCMS: t_R =3.74 min; $MH^+ = 427$. ^{19}F NMR: δ ($CDCl_3$) −79.82 and −79.88.

To a solution of the imine (185 mg, 0.43mmol) in glacial acetic acid (5 mL) stirred under nitrogen at room temperature was added sodium triacetoxyborohydride (276 mg, 1.3mmol), and the solution was stirred for approximately 4 h. Further sodium triacetoxyborohydride (100 mg, 0.47 mmol) was added, and the mixture was stirred for 1 h. The solution was then carefully added to saturated aqueous sodium carbonate, and when effervescence had ceased, the sample was extracted into ethyl acetate (×2). The combined organic layers were washed successively with saturated aqueous sodium carbonate solution, water, and finally brine/water (1:1), passed through a hydrophobic frit, and evaporated in vacuo to yield a pale-yellow oil. The crude product was purified on a 10 g silica SPE cartridge, eluting with a 0–100% dichloromethane in a heptane gradient followed by 1% methanol in dichloromethane. This gave, in order of elution, **49D2** (racemic diastereomer 2) (45 mg) and **49D1** (racemic diastereomer 1) (35 mg).

Diastereomer 1 49D1. LCMS: t_R =3.56 min; $MH^+ = 429$. ^1H NMR: δ_H ($CDCl_3$) 9.15 (s, 1H), 8.48 (d, 1H), 7.45 (d, 1H), 7.39 (d, 1H), 7.36–7.28 (m, 2H), 7.25–7.18 (m, 3H), 6.11 (d, 1H), 4.19 (m, 1H), 3.41 (s, 1H), 3.28 (t, 1H), 2.93 (dd, 1H), 2.83–2.76 (m, 2H), 2.39–2.27 (m, 3H), 1.93–1.73 (m, 4H), 1.69–1.62 (m, 1H), 0.86 (t, 3H). ^{19}F NMR: δ ($CDCl_3$) −80.36. **49D1** $C_{25}H_{28}F_3N_2O$ (MH^+): calcd 429.2154, found 429.2152.

Diastereomer 2 49D2. LCMS: t_R =3.57 min; $MH^+ = 429$. ^{19}F NMR: δ ($CDCl_3$) −81.29.

Racemic diastereomer 1 **49D1** was separated into its enantiomers using a 2 cm × 25 cm Chiralcel OD column, eluting with 10% ethanol in heptane with a flow rate of 15 mL/min. Diastereomer 1, enantiomer 1 **49D1E1** eluted around 7.0 min, and diastereomer 1, enantiomer 2 **49D1E2** eluted around 8.0 min.

49D1E1. Analytical chiral HPLC (25 cm × 0.46 cm Chiralcel OD column, 10% ethanol in heptane, eluting at 1 mL/min): $t_R = 5.26$ min. LCMS: $t_R = 3.56$ min; $MH^+ = 429$.

49D1E2. Analytical chiral HPLC (25 cm × 0.46 cm Chiralcel OD column, 10% ethanol in heptane, eluting at 1 mL/min): $t_R = 6.69$ min. LCMS: $t_R = 3.56$ min; $MH^+ = 429$. **49D1E2** $C_{25}H_{28}F_3N_2O$ (MH^+): calcd 429.2154, found 429.2155.

1,1,1-Trifluoro-3-(5-isoquinolinylamino)-2-[(1-methyl-1,2,3,4-tetrahydro-1-naphthalenyl)methyl]-2-propanol 54D1, 54D2, 54D1E1, 54D1E2, 54D2E1, 54D2E2. The imine was prepared from aldehyde **53D1+D2** and 5-isoquinolinamine **48** using a method similar to that described for **49**. LCMS: $t_R = 3.69$ and 3.74 min; $MH^+ = 413$ (40:60 ratio of diastereomers). ^{19}F NMR δ ($CDCl_3$) –79.7, −79.97 (56:44 ratio of diastereomers).

To a solution of the imine (154 mg, 0.373mmol) in glacial acetic acid (4 mL) stirred under nitrogen at 21 °C was added sodium triacetoxyborohydride (316 mg 1.5mmol) portionwise over 25 min, and the solution was stirred for a further 4 h. The solution was then carefully added to a mixture of saturated aqueous sodium carbonate (50 mL) and ethyl acetate (30 mL) and stirred for 10 min, when effervescence had ceased. The layers were separated, and the aqueous layer was re-extracted with ethyl acetate (30 mL). The combined organic layers were washed with saturated sodium carbonate (15 mL), water (2 × 30 mL), and saturated brine (30 mL), dried over anhydrous sodium sulfate, and evaporated. The crude product was purified on a 50 g silica cartridge using a Flashmaster 2 system with a 0–100% gradient of ethyl acetate in cyclohexane over 80 min to give the title compound (92 mg, 59.5%). Early fractions were evaporated to give a pure sample of racemic diastereomer 2 **54D2** (24.8.mg), while late fractions were evaporated to give racemic diastereomer 1 **54D1** (8.7 mg).

Diastereomer 1 54D1. LCMS: $t_R = 3.48$ min; $MH^+ = 415$. ^1H NMR: δ_H ($CDCl_3$) 9.13 (s, 1H), 8.46 (d, 1H), 7.46 (d, 1H), 7.38 (d, 2H), 7.32 (t, 1H), 7.24–7.17 (m, 3H), 6.13 (d, 1H), 4.23 (m, 1H), 3.51 (bs, 1H), 3.26 (t, 1H), 2.93 (dd, 1H), 2.81 (m, 2H), 2.61–2.51 (m, 2H), 2.22 (d, 1H), 1.92–1.68 (m, 3H), 1.39 (s, 3H). ^{19}F NMR: δ (DMSO-d_6) −78.17.

Diastereomer 2 54D2. LCMS: $t_R = 3.51$ min; $MH^+ = 415$. ^1H NMR: δ_H ($CDCl_3$) 9.16 (s, 1H), 8.46 (d, 1H), 7.50–7.42 (m, 3H), 7.38 (d, 1H), 7.24–7.11 (m, 3H), 6.63 (d, 1H), 4.63 (t, 1H), 3.65–3.50 (m, 2H), 2.83–2.77 (m, 2H), 2.70–2.65 (m, 2H), 2.33–2.24 (m, 1H), 2.00 (d, 1H), 1.93–1.77 (m, 2H), 1.72–1.66 (m, 1H), 1.42 (s, 3H). ^{19}F NMR: (DMSO-d_6) −78.03.

Diastereomer 1 **54D1** (6 mg) was separated into its enantiomers using a 2 cm × 25 cm Chiralcel OD column, eluting with 10% ethanol in heptane with a flow rate of 15 mL/min. Diastereomer 1, enantiomer 1 **54D1E1** eluted around 6.8 min (1.45 mg), and diastereomer 1, enantiomer 2 **54D1E2** eluted around 9.3 min (1.31 mg).

54D1E1. Analytical chiral HPLC (25 cm × 0.46 cm Chiralcel OD column, 10% ethanol in heptane, eluting at 1 mL/min): t_R = 5.47 min. LCMS: t_R = 3.45 min; MH^+ = 415.

54D1E2. Analytical chiral HPLC (25 cm × 0.46 cm Chiralcel OD column, 10% ethanol in heptane, eluting at 1 mL/min): t_R = 7.45 min. LCMS: t_R = 3.47 min; MH^+ = 415. **54D1E2** $C_{24}H_{26}F_3N_2O$ (MH^+): calcd 415.1997, found 415.2007.

Diastereomer 2 **54D2** was separated into its enantiomers using a 2 cm × 25 cm Chiralcel OD column, eluting with 10% ethanol in heptane with a flow rate of 15 mL/min. Diastereomer 2, enantiomer 1 **54D2E1** eluted around 9.0 min, and diastereomer 2, enantiomer 2 **54D2E2** eluted around 12.5 min .

54D2E1. Analytical chiral HPLC (25 cm × 0.46 cm Chiralcel OD column, 10% ethanol in heptane, eluting at 1 mL/min): t_R = 7.69 min. LCMS: t_R = 3.51 min; MH^+ = 415. **54D2E1** $C_{24}H_{26}F_3N_2O$ (MH^+): calcd 415.1997, found 415.1992.

54D2E2. Analytical chiral HPLC (25 cm × 0.46 cm Chiralcel OD column, 10% ethanol in heptane, eluting at 1 mL/min): t_R = 10.32 min. LCMS: t_R = 3.52 min; MH^+ = 415.

1,1,1-Trifluoro-3-[(2-methyl-5-quinolinyl)amino]-2-[(1-methyl-1,2,3,4-tetrahydro-1-naphthalenyl)methyl]-2-propanol 55D1, 55D1E1, 55D1E2. The imine was prepared from the aldehydes **53D1+D2** and 2-methyl-5-quinolinamine **44** using a method similar to that described for **49**. LCMS: t_R = 3.64 and 3.73 min; MH^+ = 427 (48:52 ratio of diastereomers). ^{19}F NMR: δ ($CDCl_3$) −79.80, −80.02 (54:46 ratio of diastereomers).

To a solution of the imine (130 mg, 0.30mmol) in glacial acetic acid (4 mL) stirred under nitrogen at 21 °C was added sodium triacetoxyborohydride (254 mg, 1.2mmol) portionwise over 25 min, and the solution was stirred for a further 4 h. The solution was then carefully added to a mixture of saturated aqueous sodium carbonate (50 mL) and ethyl acetate (30 mL) and stirred for 10 min, when effervescence had finished. The layers were separated, and the aqueous layer was re-extracted with ethyl acetate (30 mL). The combined organic layers were washed with saturated sodium carbonate (15 mL), water (2 × 30 mL), and saturated brine (30 mL), dried over anhydrous sodium sulfate, and evaporated. The crude product was purified on a 50 g silica cartridge using a Flashmaster 2 system with a 0–100% gradient of ethyl acetate in cyclohexane over 80 min to give the title compound (91.6 mg, 71%) as a mixture of diastereomers. Further purification using mass-directed autopreparative reverse-phase HPLC gave racemic diastereomer 1 **55D1** (7.1 mg) and racemic diastereomer 2 **55D2** (5.5 mg).

55D1 (Racemic Diastereomer 1). LCMS t_R = 2.89 min; MH^+ = 429. ^{1}H NMR: δ_H ($CDCl_3$) 7.95 (d, 1H), 7.48 (d, 1H0, 7.38 (t, 2H), 7.25–7.17 (m, 4H), 5.96 (d, 1H), 4.11 (m, 1H), 3.40 (bs, 1H), 3.26 (t, 1H), 2.91 (dd, 1H), 2.81 (m, 2H), 2.73 (s, 3H), 2.57–2.47 (m, 2H), 2.22 (d, 1H), 1.91–1.76 (m, 2H), 1.74–1.67 (m, 1H), 1.38 (t, 3H). ^{19}F NMR: δ (DMSO-d_6) −78.16.

55D2 (Racemic Diastereomer 2). LCMS: t_R = 2.92 min; MH^+ = 429. ^{1}H NMR: δ_H (DMSO-d_6) 8.35 (d, 1H), 7.46 (t, 1H), 7.37 (d, 1H), 7.32 (d, 1H), 7.18 (d, 1H), 7.08–6.96 (m, 3H), 6.56 (d, 1H), 5.75 (m, 1H), 3.55 (m, 1H), 3.33 (s, 3H), 3.31 (m, 1H0, 2.68 (m, 2H), 2.61 (s, 3H), 2.59 (m, 1H), 2.33 (m, 1H), 2.16 (m, 2H), 1.84–1.73 (m, 1H), 1.72–1.58 (m, 2H). ^{19}F NMR: δ (DMSO-d_6) −78.07.

Diastereomer 1 **55D1** (5.6 mg) was separated into its enantiomers using a 2 cm × 25 cm Chiralpak AD column, eluting with 30% ethanol in heptane with a flow rate of 15 mL/min. Diastereomer 1, enantiomer 1 **55D1E1** eluted around 4.2 min (0.9 mg), and diastereomer 1, enantiomer 2 **55D1E2** eluted around 9.0 min (1.55 mg).

55D1E1. Analytical chiral HPLC (25 cm × 0.46 cm Chiralpak AD column, 30% ethanol in heptane, eluting at 1 mL/min): t_R = 3.32 min. LCMS: t_R = 2.95min; MH^+ = 429. **55D1E1** $C_{25}H_{28}F_3N_2O$ (MH^+): calcd 429.2154, found 429.2149.

55D1E2. Analytical chiral HPLC (25 cm × 0.46 cm Chiralpak AD column, 30% ethanol in heptane, eluting at 1 mL/min): t_R = 7.79 min. LCMS: t_R = 3.01 min; MH^+ = 429.

Diastereomer 2 **55D2** was separated into its enantiomers using a 2 cm × 25 cm Chiralpak AD column, eluting with 3% ethanol in heptane with a flow rate of 15 mL/min. Diastereomer 2, enantiomer 1 **55D2E1** eluted around 12 min, and diastereomer 2, enantiomer 2 **55D2E2** eluted around 16 min

55D2E1. Analytical chiral HPLC (25 cm × 0.46 cm Chiralpak AD column, 3% ethanol in heptane, eluting at 1 mL/min): t_R = 11.18 min. LCMS: t_R = 2.92 min; MH^+ = 429. **55D2E1** $C_{25}H_{28}F_3N_2O$ (MH^+): calcd 429.2154, found 429.2149.

55D2E2. Analytical chiral HPLC (25 cm × 0.46 cm Chiralpak AD column, 3% ethanol in heptane, eluting at 1 mL/min): t_R = 13.89 min. LCMS: t_R = 2.94 min; MH^+ = 429.

1,1,1-Trifluoro-3-(1-methyl-1,2,3,4-tetrahydro-1-naphthalenyl)-2-[(5-quinolinylamino)methyl]-2-propanol 56D1, 56D1E1, 56D1E2. A solution of the aldehydes **53D1+D2** (200 mg, 0.7 mmol) and 5-quinolinamine **42** (131 mg, 0.9mmol) in glacial acetic acid (4 mL) was microwaved at 160 °C for 30 min. The solution was added to toluene (25 mL) and evaporated, and the remaining acetic acid was azeotroped by evaporating again with toluene (50 mL). The crude product was purified on a 5 g silica Bond Elut cartridge, eluting with 1:1 cyclohexane/dichloromethane followed by a 10:1 to 3:1 gradient of cyclohexane/ethyl acetate to give the imine (177 mg, 60%). LCMS: t_R = 3.77 and 3.81 min; MH^+ = 413 (38:62 ratio of diastereomers). ^{19}F NMR: δ ($CDCl_3$) −79.78, −79.99 (57:43 ratio of diastereomers).

To a solution of the imine (172 mg, 0.417mmol) in glacial acetic acid (4 mL) stirred under nitrogen at 21 °C was added sodium triacetoxyborohydride (353 mg, 1.66 mmol) portionwise over 25 min, and the solution was stirred for a further 4 h. The solution was then carefully added to a mixture of saturated aqueous sodium carbonate (50 mL) and ethyl acetate (30 mL) and stirred for 10 min, when effervescence had finished. The layers were separated, and the aqueous layer was re-extracted with ethyl acetate (30 mL). The combined organic layers were washed with saturated sodium carbonate (15 mL), water (2 × 30 mL), and saturated brine (30 mL), dried over anhydrous sodium sulfate, and evaporated. The crude product was purified on a 50 g silica cartridge using a Flashmaster 2 system with a 0–100% gradient of ethyl acetate in cyclohexane over 40 min to give the title compound (74.3 mg, 43%) as a mixture of diastereomers. Further purification using mass-directed autopreparative reverse-phase HPLC gave racemic diastereomer 1 **56D1** (10 mg) and racemic diastereomer 2 **56D2** (8.9 mg).

56D1 Diastereomer 1. LCMS: t_R = 3.35 min; MH^+ = 415. ^{1}H NMR: δ_H (DMSO-d_6) 8.78 (dd, 1H), 8.33 (d, 1H), 7.48 (d, 1H), 7.41 (dd, 1H), 7.33 (t, 1H), 7.22–7.15 (m, 2H), 7.12–7.05 (m, 2H), 6.17 (s, 1H), 5.87 (d, 1H), 5.55 (m, 1H), 3.00 (d, 1H), 2.85 (dd, 1H), 2.69 (m, 2H), 2.60–2.50 (m, 2H), 2.04 (d, 1H), 1.85–1.77 (s, 1H), 1.75–1.61 (m, 2H), 1.31 (s, 3H). ^{19}F NMR: δ (DMSO-d_6) −78.16.

56D2 Diastereomer 2. LCMS: t_R = 3.42 min; MH^+ = 415. ^{19}F NMR: δ (DMSO-d_6) −78.05.

Diastereomer 1 **56D1** was separated into its enantiomers using a 2 cm × 25 cm Chiralpak AD column, eluting with 60% ethanol in heptane with a flow rate of 15 mL/min. Diastereomer 1, enantiomer 1 **56D1E1** eluted around 3.5 min, and diastereomer 1, enantiomer 2 **56D1E2** eluted around 7 min

56D1E1 (Enantiomer 1 of Diastereomer 2). Analytical chiral HPLC (25 cm × 0.46 cm Chiralpak AD column, 60% ethanol in heptane, eluting at 1 mL/min): t_R = 3.15 min. LCMS: t_R = 3.32 min; MH^+ = 415. **56D1E1** $C_{28}H_{31}F_3NO$ (MH^+): calcd 454.2358, found 454.2364.

56D1E2 (Enantiomer 2 of Diastereomer 2). Analytical chiral HPLC (25 cm × 0.46 cm Chiralpak AD column, 60% ethanol in heptane, eluting at 1 mL/min): $t_R = 5.68$ min. LCMS: $t_R = 3.37$ min; MH^+ 415

Acknowledgment. We thank Ryan P Trump and Eugene Stewart for helpful discussions, particularly regarding the mutation studies.

Supporting Information Available: Additional experimental and spectroscopic data for various analogues are detailed. This material is available free of charge via the Internet at http://pubs.acs.org.

References

(1) Schimmer, B. P.; Parker, K. L. Adrenocorticotropic Hormone. Adrenocortical Steroids and Their Synthetic Analogues: Inhibitors of the Synthesis and Actions of Adrenocortical Hormones. In *Goodman and Gilman's The Pharmacological Basis of Therapeutics*, 10th ed.; Hardman, J. G., Limbird, L. E., Gilman, A. G., Eds.; McGraw-Hill: New York, 2001; pp 1649–1677.

(2) Buttgereit, F.; Straub, R. H.; Wehling, M.; Burmester, G.-R. Glucocorticoids in the Treatment of Rheumatic Disease. *Arthritis Rheum.* **2004**, *50*, 3408–3417.

(3) Schacke, H.; Docke, W. D.; Asdullah, K. Mechanisms Involved in the Side Effects of Glucocorticoids. *Pharmacol. Ther.* **2002**, *96*, 23–43.

(4) Resche-Rigon, M.; Gronemeyer, H. Therapeutic potential of selective modulators of nuclear receptor action. *Curr. Opin. Chem. Biol.* **1998**, *2*, 501–507. Barnes, P. J. Anti-inflammatory actions of glucocorticoids: molecular mechanisms. *Clin. Sci.* **1998**, *94*, 557–572. Buckbinder, L.; Robinson, R. P. The Glucocorticoid Receptor: Molecular Mechanism and New Therapeutic Opportunities. *Curr. Drug Targets: Inflammation Allergy* **2002**, *1*, 127–136.

(5) Abbott/Ligand. For leading references, see the following: Ardecky, R. J.; Hudson, A. R.; Phillips, D. P.; Tyhonas, J. S.; Deckhut, C.; Lau, T. L.; Li, Y.; Martinborough, E. A.; Roach, S. L.; Higuchi, R. I.; Lopez, F. J.; Marschke, K. B.; Miner, J. N.; Karanewsky, D. S.; Negro-Vilar, A.; Zhi L. 5(*Z*)-Benzylidene-1,2-dihydro-9-hydroxy-10-methoxy-2,2,4-trimethyl-5*H*-1-aza-6-oxa-chrysenes as non-steroidal glucocorticoid receptor modulators. *Bioorg. Med. Chem. Lett.*, in press. Elmore, S. W.; Coghlan, M. J.; Anderson, D. D.; Pratt, J. K.; Green, B. E.; Wang, A. X.; Stashko, M. A.; Lin, C. W.; Tyree, C. M.; Miner, J. N.; Jacobson, P. B.; Wilcox, D. M.; Lane, B. C. Nonsteroidal Selective Glucocorticoid Modulators: The Effect of C-5 Alkyl Substitution on the Transcriptional Activation/Repression Profile of 2,5-Dihydro-10-methoxy-2,2,4-trimethyl-1*H*-[1]benzopyrano[3,4-*f*]quinolines. *J. Med. Chem.* **2001**, *44*, 4481–4491. Kym, P. R.; Kort, M. E.; Coghlan, M. J.; Moore, J. L.; Tang, R.; Ratajczyk, J. D.; Larson, D. P.; Elmore, S. W.; Pratt, J. K.; Stashko, M. A.; Falls, H. D.; Lin, C. W.; Nakane, M.; Miller, L.; Tyree-Curtis, M.; Miner, J. N.; Jacobson, P. B.; Wilcox, D. M.; Nguyen, P.; Lane, B. C. Nonsteroidal Selective Glucocorticoid Modulators: The Effect of C-10 Substitution on Receptor Selectivity and Functional Potency of 5-Allyl-2,5-dihydro-2,2,4-trimethyl-1*H*-[1]benzopyrano[3,4-*f*]quinolines. *J. Med. Chem.* **2003**, *46*, 1016–1030, and references therein. Elmore, S. W.; Pratt, J. K.; Coghlan, M. J.; Mao, Y.; Green, B. E.; Anderson, D. D.; Stashko, M. A.; Lin, C. W.; Falls, D.; Nakane, M.; Miller, L.; Tyree, C. M.; Miner, J. N.; Lane, B. Differentiation of in Vitro Transcriptional Repression and Activation Profiles of Selective Glucocorticoid Modulators. *Bioorg. Med. Chem. Lett.* **2004**, *14*, 1721–1727.

(6) Schering. Schacke, H.; Schottelius, A.; Docke, W.-D.; Strehlke, P.; Jaroch, S.; Schmees, N.; Rehwinkel, H.; Hennekes, H.; Asadullah, K. Dissociation of transactivation from transrepression by a selective glucocorticoid receptor agonist leads to separation of therapeutic effects from side effects. *Proc. Nat. Acad. Sci. U.S.A.* **2004**, *101*, 227–32. Jaroch, S.; Rehwinkel, H.; Schacke, H.; Schmees, N.; Skuballa, W.; Schneider, M.; Hubner, J.; Petrov, O. 5-Substituted Quinoline and Isoquinoline Derivatives, a Method for the Production Thereof and Their Use as Antiphlogistics. *PCT Int. Appl.* WO 050998, 2006.

(7) Merck. For leading references, see the following: Thompson, C. F.; Quraishi, N.; Ali, A.; Mosley, R. T.; Tata, J. R.; Hammond, M. L.; Balkovec, J. M.; Einstein, M.; Ge, L.; Harris, G.; Kelly, T. M.; Mazur, P.; Pandit, S.; Santoro, J.; Sitlani, A.; Wang, C.; Williamson, J.; Miller, D. K.; Yamin, T. D.; Thompson, C. M.; O'Neill, E. A.; Zaller, D.; Forrest, M. J.; Carballo-Jane, E.; Luell, S. Novel Glucocorticoids Containing a 6,5-Bicyclic Core Fused to a Pyrazole Ring: Synthesis, in Vitro Profile, Molecular Modeling Studies, and in Vivo Experiments. *Bioorg. Med. Chem. Lett.* **2007**, *17*, 3354–3361. Ali, A.; Thompson, C. F.; Balkovec, J. M.; Graham, D. W.; Hammond, M. L.; Quraishi, N.; Tata, J. R.; Einstein, M.; Ge, L.; Harris, G.; Kelly, T. M.; Mazur, P.; Pandit, S.; Santoro, J.; Sitlani, A.; Wang, C.; Williamson, J.; Miller, D. K.; Thompson, C. M.; Zaller, D. M.; Forrest, M. J.; Carballo-Jane, E.; Luell, S. Novel *N*-Arylpyrazolo[3,2-*c*]-Based Ligands for the Glucocorticoid Receptor: Receptor Binding and in Vivo Activity. *J. Med. Chem.* **2004**, *47*, 2441–2452. Thompson, C. F.; Quraishi, N.; Ali, A.; Tata, J. R.; Hammond, M. L.; Balkovec, J. M.; Einstein, M.; Ge, L.; Harris, G.; Kelly, T. M.; Mazur, P.; Pandit, S.; Santoro, J.; Sitlani, A.; Wang, C.; Williamson, J.; Miller, D. K.; Yamin, T. D.; Thompson, C. M.; O'Neill, E. A.; Zaller, D.; Forrest, M. J.; Carballo-Jane, E.; Luell, S. Novel Heterocyclic Glucocorticoids: In Vitro Profile and in Vivo Efficacy. *Bioorg. Med. Chem. Lett.* **2005**, *15*, 2163–2167. Smith, C. J.; Ali, A.; Balkovec, J. M.; Graham, D. W.; Hammond, M. L.; Patel, G. F.; Rouen, G. P.; Smith, S. K.; Tata, J. R.; Einstein, M.; Ge, L.; Harris, G. S.; Kelly, T. M.; Mazur, P.; Thompson, C. M.; Wang, C. F.; Williamson, J. M.; Miller, D. M.; Pandit, S.; Santoro, J. C.; Sitlani, A.; Yamin, T. D.; O'Neill, E. A.; Zaller, D. M.; Carballo-Jane, E.; Forrest, M. J.; Luell, S. Novel Ketal Ligands for the Glucocorticoid Receptor: In Vitro and in Vivo Activity. *Bioorg. Med. Chem. Lett.* **2005**, *15*, 2926–2931.

(8) Boehringer Ingelheim. For leading references, see the following: Regan, J.; Lee, T. W.; Zindell, R. M.; Bekkali, Y.; Bentzien, J.; Gilmore, T.; Hammach, A.; Kirrane, T. M.; Kukulka, A. J.; Kuzmich, D.; Nelson, R. M.; Proudfoot, J. R.; Ralph, M.; Pelletier, J.; Souza, D.; Zuvela-Jelaska, L.; Nabozny, G.; Thomson, D. S. Quinol-4-ones as Steroid A-Ring Mimetics in Nonsteroidal Dissociated Glucocorticoid Agonists. *J. Med. Chem.* **2006**, *49*, 7887–7896. Betageri, R.; Zhang, Y.; Zindell, R. M.; Kuzmich, D.; Kirrane, T. M.; Bentzien, J.; Cardozo, M.; Capolino, A. J.; Fadra, T. N.; Nelson, R. M.; Paw, Z.; Shih, D.-T.; Shih, C.-K.; Zuvela-Jelaska, L.; Nabozny, G.; Thomson, D. S. Trifluoromethyl Group as a Pharmacophore: Effect of Replacing a CF_3 Group on Binding and Agonist Activity of a Glucocorticoid Receptor Ligand. *Bioorg. Med. Chem. Lett.* **2005**, *15*, 4761–4769. Marshall, D. R. 3-Sulfonamidoethylindole Derivatives for Use as Glucocorticoid Mimetics in the Treatment of Inflammatory, Allergic and Proliferative Diseases *PCT Int. Appl.* WO 019935, 2004. Other patents include WO 2003 059899, 082280, 082787, 101932, 104195, WO 2004 018429, 063163, 075864.

(9) University of California. Shah, N.; Scanlan, T. S. Design and Evaluation of Novel Nonsteroidal Dissociating Glucocorticoid Receptor Ligands. *Bioorg. Med. Chem. Lett.* **2004**, *14*, 5199–5203.

(10) Karo Bio/Abbott. Kauppi, B.; Jakob, C.; Farnegardh, M.; Yang, J.; Ahola, H.; Alarcon, M.; Calles, K.; Engstrom, O.; Harlan, J.; Muchmore, S.; Ramqvist, A.-K.; Thorell, S.; Ohman, L.; Greer, J.; Gustafsson, J.-A.; Carlstedt-Duke, J.; Crlquist, M. The Three-dimensional Structures of Antagonistic and Agonistic Forms of the Glucocorticoid Receptor Ligand-Binding Domain. *J. Biol. Chem.* **2003**, 22748–22754. Link, J. T.; Sorensen, B. K.; Lai, C.; Wang, J.; Fung, S.; Deng, D.; Emery, M.; Carroll, S.; Grynfarb, M.; Goos-Nilsson, A.; von Geldern, T. Synthesis, Activity, Metabolic Stability and Pharmacokinetics of Glucocorticoid Receptor Modulator-Statins Hybrids. *Bioorg. Med. Chem. Lett.* **2004**, *14*, 4173–4178, and references therein.

(11) Pfizer. Morgan, B. P.; Liu, K.K.-C.; Dalvie, D. K.; Swick, A. G.; Hargrove, D. M.; Wilson, T. C.; LaFlamme, J. A.; Moynihan, M. S.; Rushing, M. A.; Woodworth, G. F.; Li, J.; Trilles, R. V.; Yang, X.; Harper, K. W.; Carroll, R. S.; Martin, K. A.; Nardone, N. A.; O'Donnell, J. P.; Faletto, M. B.; Vage, C.; Soliman, V. Discovery of Potent, Non-Steroidal and Highly Selective Glucocorticoid Receptor Antagonists with Anti-Obesity Activity. *Lett. Drug Des. Discovery* **2004**, *1*, 1–5.

(12) Barker, M.; Clackers, M.; Demaine, D. A.; Humphreys, D.; Johnston, M. J.; Jones, H. T.; Pacquet, F.; Pritchard, J. M.; Shanahan, S. E.; Skone, P. A.; Vinader, V. M.; Uings, I.; McLay, I. M.; Macdonald, S.J.F. Design and Synthesis of New Non-Steroidal Glucocorticoid Modulators through Application of an "Agreement Docking" Method. *J. Med. Chem.* **2005**, *48*, 4507–4510.

(13) Barker, M. D.; Demaine, D. A.; House, D.; Inglis, G.G.A.; Johnston, M. J.; Jones, H. T.; Macdonald, S. J. F.; McLay, I. M.; Shanahan, S.; Skone, P. A.; Vinader, M. V. Preparation of Heterocycle-Substituted *N*-Benzoxazinylpropanamides as Glucocorticoid Receptor Binders and Agonists for the Treatment of Inflammatory, Allergic and Skin Diseases. *PCT Int. Appl.* WO 071389, 2004.

(14) Barker, M.; Clackers, M.; Copley, R.; Demaine, D. A.; Humphreys, D.; Inglis, G.G.A.; Johnston, M. J.; Jones, H. T.; Haase, M. V.; House, D.; Loiseau, R.; Nisbet, L.; Pacquet, F.; Skone, P. A.; Shanahan, S. E.; Tape, D.; Vinader, V. M.; WA, M.; Uings, I.; Upton, R.; McLay, I. M.; Macdonald, S.J.F. Dissociated Non-Steroidal Glucocorticoid Receptor Modulators; Discovery of the Agonist Trigger in a Tetrahydronaphthalene–Benzoxazine Series. *J. Med. Chem.* **2006**, *49*, 4216–4231.

(15) Bledsoe, R. K.; Montana, V. G.; Stanley, T. B.; Delves, C. J.; Apolito, C. J.; McKee, D. D.; Consler, T. G.; Parks, D. J.; Stewart, E. L.;

Willson, T. M.; Lambert, M. H.; Moore, J. T.; Pearce, K. H.; Xu, H. E. Crystal Structure of the Glucocorticoid Receptor Ligand Binding Domain Reveals a Novel Mode of Receptor Dimerization and Coactivator Recognition. *Cell* **2002**, *110*, 93–105.

(16) Weingarten, G. G.; Biggadike, K.; Jack, T. I.; Jones, P. S.; Harker, A. J.; Taylor, S. J.; Vince, P.; Clackers, M. Betamethasone 17α-Carbamates As Potent, Dissociated Glucocorticoid Receptor Agonists. Presented at the 229th National Meeting of the American Chemical Society, San Diego, CA, March 13–17, 2005; MEDI-161.

JM070778W